A reverse signaling pathway downstream of Sema4A controls cell migration via Scrib

Tianliang Sun,[1] Lida Yang,[1] Harmandeep Kaur,[1] Jenny Pestel,[1] Mario Looso,[1] Hendrik Nolte,[1] Cornelius Krasel,[2] Daniel Heil,[1] Ramesh K. Krishnan,[1] Marie-Josée Santoni,[4,5,6,7] Jean-Paul Borg,[4,5,6,7] Moritz Bünemann,[2] Stefan Offermanns,[1,8] Jakub M. Swiercz,[1]* and Thomas Worzfeld[1,3]*

[1]Max Planck Institute for Heart and Lung Research, 61231 Bad Nauheim, Germany
[2]Institute of Pharmacology and Clinical Pharmacy and [3]Institute of Pharmacology, Biochemical-Pharmacological Center, University of Marburg, 35043 Marburg, Germany
[4]Cell Polarity, Cell Signaling and Cancer, Equipe labellisée Ligue Contre le Cancer, Institut National de la Santé et de la Recherche Médicale, U1068, 13009 Marseille, France
[5]Institut Paoli-Calmettes, 13009 Marseille, France
[6]Aix-Marseille Université, 13284 Marseille, France
[7]Centre National de la Recherche Scientifique, UMR7258, 13273 Marseille, France
[8]Medical Faculty, University of Frankfurt, 60590 Frankfurt am Main, Germany

Semaphorins comprise a large family of ligands that regulate key cellular functions through their receptors, plexins. In this study, we show that the transmembrane semaphorin 4A (Sema4A) can also function as a receptor, rather than a ligand, and transduce signals triggered by the binding of Plexin-B1 through reverse signaling. Functionally, reverse Sema4A signaling regulates the migration of various cancer cells as well as dendritic cells. By combining mass spectrometry analysis with small interfering RNA screening, we identify the polarity protein Scrib as a downstream effector of Sema4A. We further show that binding of Plexin-B1 to Sema4A promotes the interaction of Sema4A with Scrib, thereby removing Scrib from its complex with the Rac/Cdc42 exchange factor βPIX and decreasing the activity of the small guanosine triphosphatase Rac1 and Cdc42. Our data unravel a role for Plexin-B1 as a ligand and Sema4A as a receptor and characterize a reverse signaling pathway downstream of Sema4A, which controls cell migration.

Introduction

Semaphorins are a large family of secreted, transmembrane, or glycosylphosphatidylinositol-linked proteins defined by a semaphorin domain (Kolodkin et al., 1993; Luo et al., 1993). They exert most of their effects through a family of transmembrane receptors, called plexins (Winberg et al., 1998; Tamagnone et al., 1999). Semaphorins and plexins have been shown to play crucial roles in a multitude of biological contexts, including the nervous, immune, bone, and cardiovascular systems, as well as in cancer (Takamatsu and Kumanogoh, 2012; Gu and Giraudo, 2013; Messina and Giacobini, 2013; Worzfeld and Offermanns, 2014). In various cell types, semaphorin–plexin signaling regulates key cellular functions, particularly cytoskeletal dynamics and cell migration (Kruger et al., 2005; Casazza et al., 2007).

On the basis of phylogenetic tree analysis and the presence of additional protein motifs, mammalian semaphorins are grouped into five classes. Class 3 semaphorins are secreted molecules, the class 7 semaphorin, semaphorin 7A (Sema7A), is glycosylphosphatidylinositol linked to the membrane, and semaphorins of classes 4, 5, and 6 represent transmembrane proteins (Worzfeld and Offermanns, 2014). The extracellular portion of class 4 semaphorins can be proteolytically cleaved, allowing them to also act as soluble ligands (Wang et al., 2001; Hemming et al., 2009; Fong et al., 2011; Armendáriz et al., 2012; Nakatsuji et al., 2012). Importantly, all class 4 semaphorins possess short (between 57 and 149 amino acids) cytoplasmic domains, which, in the case of Sema4B, 4C, 4F, and 4G, have been shown to interact with intracellular proteins, including PSD-95 (Inagaki et al., 2001; Burkhardt et al., 2005), SEM CAP-1 and -2 (GIPC1/2; Wang et al., 1999), Norbin (Ohoka et al., 2001), and CLCP1 (Nagai et al., 2007). Plexins, in turn,

*J.M. Swiercz and T. Worzfeld contributed equally to this paper.

Correspondence to Tianliang Sun: tianliang.sun@mpi-bn.mpg.de; or Thomas Worzfeld: thomas.worzfeld@staff.uni-marburg.de

H. Nolte's present address is Institute for Genetics and Cologne Excellence Cluster on Cellular Stress Responses in Aging-Associated Diseases, University of Cologne, 50931 Cologne, Germany.

R.K. Krishnan's present address is Dept. of Internal Medicine, Excellence Cluster in Cardio-Pulmonary Systems, University of Giessen and Marburg Lung Center, 35392 Giessen, Germany.

Abbreviations used: BMDC, bone marrow–derived DC; DC, dendritic cell; FRET, Förster resonance energy transfer; GEF, guanine nucleotide exchange factor; GM-CSF, granulocyte–macrophage colony-stimulating factor; HMVEC, human microvascular endothelial cell; PE, phycoerythrin; RIPA, radioimmunoprecipitation assay.

The Rockefeller University Press $30.00
J. Cell Biol. Vol. 216 No. 1 199–215
https://doi.org/10.1083/jcb.201602002

are classified into four subfamiles, A–D, according to structural characteristics (Tamagnone et al., 1999).

Although it is well established that the binding of semaphorins to plexins triggers several plexin-mediated signaling pathways (Hota and Buck, 2012; Jongbloets and Pasterkamp, 2014), it remains largely unclear whether transmembrane semaphorins can also serve as receptors, rather than ligands, and signal in a reverse manner (Gurrapu and Tamagnone, 2016). Several studies in the developing nervous system of *Drosophila melanogaster* provide evidence that Sema1a, a transmembrane semaphorin found in invertebrates, transduces signals evoked by binding of plexins, which depend on the intracellular domain of Sema1a (Godenschwege et al., 2002; Cafferty et al., 2006; Komiyama et al., 2007; Yu et al., 2010). In vertebrates, a receptor function has been assigned to Sema6B, which controls axon guidance in the developing chick nervous system (Andermatt et al., 2014). Moreover, it has been suggested that murine Plexin-B2 regulates epidermal γδ T cell functions through Sema4D (Witherden et al., 2012). However, the underlying molecular mechanisms remain elusive.

In this study, we show that Sema4A serves as a receptor for Plexin-B1 and mediates Plexin-B1–induced reverse signaling. Mechanistically, we uncover Scrib as a critical mediator of Sema4A downstream signaling in cancer and dendritic cells (DCs). Sema4A interacts with Scrib in a Plexin-B1–dependent manner, resulting in decreased membrane localization of Scrib and a loss of the interaction between Scrib and the guanine nucleotide exchange factor βPIX, thus negatively regulating the activity of the small GTPases Cdc42 and Rac1. Furthermore, we provide evidence that this Sema4A–Scrib–βPIX signaling pathway is critical to promote Plexin-B1–induced migration and invasion of various cancer cells as well as the migration of DCs.

Results

Plexin-B1 induces migration and invasion of cancer cells via Sema4A reverse signaling

Class 4 semaphorins and B-family plexins have been linked to the regulation of the cytoskeleton and cell migration (Driessens et al., 2001; Swiercz et al., 2008). To test whether class 4 semaphorins can act as receptors, rather than ligands, in the context of cancer cell migration, we purified an extracellular portion of Plexin-B1 containing semaphorins and a plexin-semaphorin-integrin (PSI) domain (ecPlxnB1). In accordance with published data, ecPlxnB1 contained all structural elements required for the binding to the class 4 semaphorin, Sema4D (Fig 1 a; Janssen et al., 2010). In a panel of cancer cell lines of different origin, comprising pancreatic (MIA PaCa-2, AsPc, T3M4, and CFP AC), skin (A431), brain (SHSY-5Y), cervical (HeLa), breast (MDA-MB-231), and lung (Calu-3) cancer cell lines, we observed that ecPlxnB1 increased the migratory behavior of some, but not all, cancer cell lines (Figs. 1 b and S1 a). We hypothesized that this was caused by a class 4 semaphorin, which acts as an ecPlxnB1 receptor and is present on responsive cell lines but absent from unresponsive cell lines. We therefore systematically analyzed the expression of class 4 semaphorins in the cancer cell lines and found that only Sema4A fulfilled these criteria (Figs. 1 c and S1 b). Of note, Sema4A has been shown to bind to Plexin-B1 (Yukawa et al., 2010). To test whether the ecPlxnB1-induced effects on cancer cell migration are mediated by Sema4A, we silenced Sema4A expression by siRNA in ecPlxnB1-responsive cell lines (Fig. S1, c and d). Indeed, knockdown of Sema4A, but not of other class 4 semaphorins, suppressed ecPlxnB1-induced migratory behavior (Fig. 1 d). To test whether the intracellular portion of Sema4A is required to transduce signals triggered by the binding of ecPlxnB1 to Sema4A, we silenced endogenous Sema4A by siRNA, followed by overexpression of siRNA-resistant wild-type Sema4A or of siRNA-resistant mutant Sema4A lacking the intracellular portion (Sema4AΔC). Both wild-type and mutant Sema4A were expressed at comparable levels (Fig. S1 e), reached the plasma membrane, and bound ecPlxnB1 in a similar manner (Fig. S1, f and g). Whereas expression of wild-type Sema4A rendered cells fully responsive to the promigratory effects of ecPlxnB1, expression of Sema4AΔC did not (Figs. 1 e and S1 h). Moreover, we engineered MIA PaCa-2 cells to stably express shRNA directed against endogenous Sema4A as well as cDNAs encoding shRNA-resistant versions of either wild-type or mutant Sema4A (Sema4AΔC; Fig. S1 i). Although cells expressing wild-type Sema4A showed an increase in invasive behavior in response to ecPlxnB1, cells expressing Sema4AΔC lacked the proinvasive response to ecPlxnB1 (Fig. 1 f). Of note, cells expressing wild-type or mutant Sema4A (Sema4AΔC) showed similar rates of proliferation (Fig. S1 j). Moreover, we observed that AsPc cells, which do not express endogenous Sema4A and do not normally respond to ecPlxnB1, become migratory in response to ecPlxnB1 upon expression of wild-type Sema4A, but not of the Sema4AΔC mutant (Fig. S1 k). Collectively, these data indicate that Sema4A can act as a receptor for Plexin-B1 and signals through its intracellular portion to promote cancer cell migration and invasion.

Sema4A reverse signaling in DCs induces directional migration toward Plexin-B1

To test for a wider biological significance of Plexin-B1–Sema4A reverse signaling, we extended our analyses to another biological system. Because Sema4A was reported to be highly expressed by bone marrow–derived DCs (BMDCs) and splenic DCs (Kumanogoh et al., 2002), we tested whether Sema4A could serve as a receptor for Plexin-B1 also on these cells. Indeed, we observed that primary BMDCs exhibited chemotaxis toward ecPlxnB1 (Fig. 2 a). Similarly, ecPlxnB1 also attracted primary splenic DCs (Fig. S2 a) in transwell migration and 3D chemotaxis assays (Figs. 2 b and S2 b). To examine whether these ecPlxnB1-induced effects on DC migration are mediated by Sema4A reverse signaling, we used Sema4A-deficient mice (Figs. 2 d and S2 c; Xia et al., 2015) from which we isolated BMDCs. Indeed, we found that BMDCs lacking Sema4A showed no directed migration toward ecPlxnB1 (Fig. 2 c). This was not caused by a general defect in cell motility, as Sema4A-deficient BMDCs reacted normally to the promigratory chemokine CCL19 (Fig. 2 c) and exhibited similar motility as wild-type BMDCs (Fig. S2 e). Reexpression of wild-type Sema4A, but not of Sema4AΔC, rescued the ability of DCs to respond to ecPlxnB1 (Fig. 2 d). These results show that Sema4A serves as a receptor for Plexin-B1 on DCs to promote chemotaxis via reverse signaling.

The migration of DCs toward lymphatic vessels requires Sema4A and Plexin-B1

To assess the physiological relevance of Sema4A reverse signaling in DCs, we analyzed the migratory behavior of DCs toward lymphatic vessels of explanted ear sheets of mice. Compared

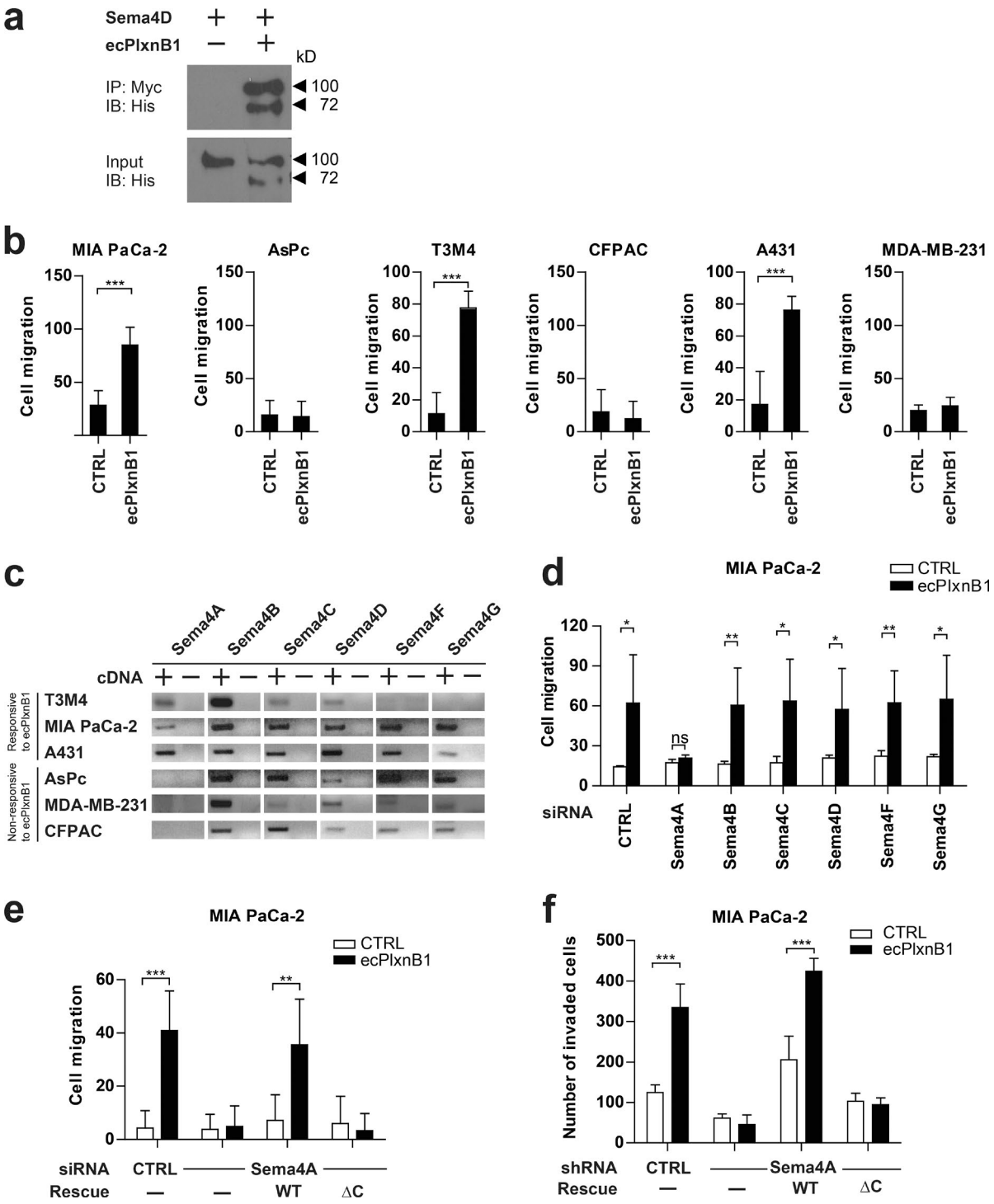

Figure 1. **Plexin-B1 promotes cancer cell migration and invasion through its receptor Sema4A.** (a) A purified His-Myc–tagged extracellular portion of Plexin-B1 (ecPlxnB1; amino acids 20–534 of human Plexin-B1) and His-tagged Sema4D were mixed in equimolar concentrations and incubated in the presence of anti-Myc antibodies. Protein complexes were then precipitated using protein A/G agarose. Proteins were immunoblotted and visualized using an anti-His antibody. IB, immunoblotting; IP, immunoprecipitation. (b) MIA PaCa-2, AsPc, T3M4, CFPAC, A431, or MDA-MB-231 cells were seeded onto 96-transwell migration plates in the absence or presence of 150 nM ecPlxnB1, and cell migration was analyzed as described in Materials and methods. Shown are mean values ± SD from duplicates of three independent experiments (total $n = 6$ per condition). CTRL, control. (c) Expression analysis of class 4 semaphorins in cancer cell lines by RT-PCR. (d) MIA PaCa-2 cells were transfected with control or siRNA directed against Sema4A, B, C, D, F, or G (as indicated). Cell migration in the absence or presence of 150 nM ecPlxnB1 was tested using a transwell system as described in Materials and methods. Shown are mean values ± SD of three independent experiments (total $n = 5$ per condition). ns, not significant. (e) MIA PaCa-2 cells were transfected with control or Sema4A siRNA. After 48 h, cells were transfected with cDNA encoding siRNA-resistant wild-type or mutant Sema4A lacking the intracellular part. Cell migration was tested using a transwell system. Shown are mean values ± SD from duplicates of three independent experiments (total $n = 6$ per condition). (f) MIA PaCa-2 cells were stably transfected with either control shRNA or shRNA against Sema4A. Where indicated, cells were additionally transfected with cDNA encoding shRNA-resistant wild-type Sema4A (WT) or shRNA-resistant Sema4A lacking its intracellular portion (ΔC). Cells were seeded onto Matrigel-coated filters (total $n = 6$ per condition). Invaded cells were stained and counted. Error bars represent means ± SD. *, $P < 0.05$; **, $P < 0.01$; ***, $P < 0.001$.

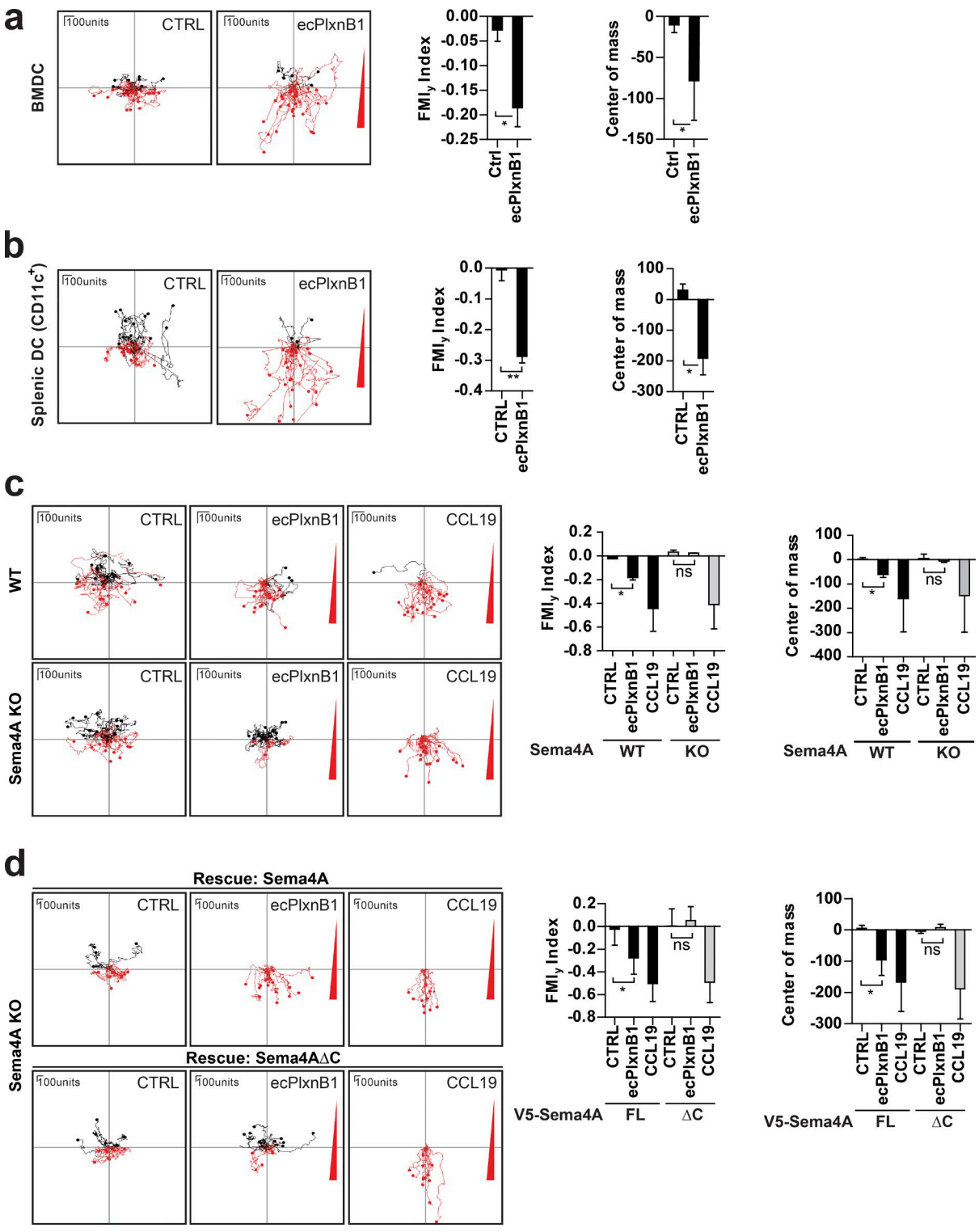

Figure 2. **Plexin-B1–Sema4A reverse signaling regulates DC migration in vitro.** (a–d) The migratory behavior of mature BMDCs (a, c, and d) or splenic DCs (b) exposed to control buffer (CTRL), to a gradient of ecPlxnB1, or to a gradient of CCL19 was analyzed as described in Materials and methods. Gradients are indicated by a red triangle at the right side of the depicted plots. Each line represents a track of an individual cell. Cell tracks with an endpoint in the top half of the plot (i.e., on the side of the lower agonist concentration) are labeled in black, and cell tracks with an endpoint in the bottom half of the plot (i.e., on the side of the higher agonist concentration) are labeled in red. (c) Mature BMDCs generated from wild-type (WT) or Sema4A knockout (KO) mice were examined. ns, not significant. (d) BMDCs isolated from Sema4A knockout mice were infected with lentiviruses carrying full-length wild-type Sema4A (V5-Sema4A FL) or Sema4A lacking the intracellular part (V5-Sema4AΔC). After maturation, cell migration was analyzed. FMI_y, y-forward migration index. Total numbers of analyzed cells are CTRL, $n = 57$ and ecPlxnB1, $n = 51$ (a); CTRL, $n = 32$ and ecPlxnB1, $n = 60$ (b); WT/CTRL, $n = 47$; WT/ecPlxnB1, $n = 38$; WT/CCL19, $n = 43$; KO/CTRL, $n = 36$; KO/ecPlxnB1, $n = 30$; and KO/CCL19, $n = 40$ (c); and FL/CTRL, $n = 26$; FL/ecPlxnB1, $n = 34$; FL/CCL19, $n = 25$; ΔC/CTRL, $n = 26$; ΔC/ecPlxnB1, $n = 33$; and ΔC/CCL19, $n = 31$ (d). Error bars represent means ± SD. *, $P < 0.05$; **, $P < 0.01$.

with wild-type BMDCs, Sema4A-deficient BMDCs were impaired in their ability to migrate toward ear lymphatic vessels (Figs. 3 a and S3 a). Given that lymphatic endothelial cells play an important role in guiding DCs to lymphatic vessels (Heuzé et al., 2013; Platt and Randolph, 2013), they seemed to be a likely source of Plexin-B1 to attract DCs via activation of Sema4A reverse signaling. Indeed, Plexin-B1 is not only expressed in arterial cells and human microvascular endothelial cells (HMVECs; Basile et al., 2005; Giusti et al., 2006), but also in lymphatic endothelial cells (Fig. S3 b; Nelson et al., 2007). Moreover, an extracellular portion of Plexin-B1 of ∼70 kD in size is released from lymphatic endothelial cells (HMVEC-dLyAd; Fig. S3, c and d). Fully consistent with a role of Plexin-B1 as a ligand for Sema4A on DCs, BMDCs were impaired in their ability to migrate toward ear lymphatic vessels of Plexin-B1–deficient mice (Fig. 3 b). The knockout of Plexin-B1 in ear lymphatic vessels led to a slightly stronger impairment of BMDC migration than the knockout of Sema4A in BMDCs (Fig. 3, a and b). Therefore, although Sema4A accounted for a large fraction of the Plexin-B1–induced promigratory effect on BMDCs, other transmembrane semaphorins could serve as additional receptors for Plexin-B1 on BMDCs. Indeed, Sema4D is coexpressed with Sema4A in BMDCs (Fig. S3, e and f). To examine the role of Sema4A reverse signaling in BMDC migration in more detail, we used a live-cell imaging approach (Video 1). This analysis showed that the migration speed and distance of Sema4A-deficient BMDCs were lower than of wild-type BMDCs (Fig. 3, c–e). However, these differences were rather subtle and therefore unlikely to fully explain the observed impairment of Sema4A-deficient BMDCs to migrate toward lymphatic vessels. Against the background of our in vitro experiments, which had shown a defective chemotactic behavior of Sema4A-deficient BMDCs toward a Plexin-B1 gradient, we hypothesized that Sema4A-deficient BMDCs might display an altered directionality of migration toward Plexin-B1–expressing lymphatic vessels. For individual cells, we therefore determined the angle between the shortest possible distance to the lymphatic vessel and the observed actual vector of migration (Fig. 3 f). Indeed, we found that Sema4A-deficient BMDCs migrated at higher angles (i.e., less directly toward lymphatic vessels) than wild-type BMDCs (Fig. 3 f).

Identification of downstream effectors of Sema4A

Our data show that the intracellular portion of Sema4A is crucial to mediate reverse signaling. To further elucidate the signaling pathway downstream of activated Sema4A, our goal was to identify proteins that interact with its intracellular portion. We therefore expressed the recombinant intracellular portion of Sema4A, incubated it with lysates of various cell lines (MIA PaCa-2, SK-OV-3, HEK293T, and CaD2), and, after precipitation, identified binding partners by mass spectrometry (Fig. 4 a). An analogous approach was taken for all other class 4 semaphorins (not depicted). As Plexin-B1–Sema4A reverse signaling promotes cell migration, we reasoned that the functional relevance of Sema4A-interacting proteins could be assessed by testing their involvement in this promigratory effect. We therefore silenced the expression of individual candidates by siRNA in MIA PaCa-2 cells and tested for the impact on ecPlxnB1-induced cell migration. The knockdown of several Sema4A-interacting proteins severely impaired the ability of cells to respond to ecPlxnB1, with the knockdown of Scrib having the strongest effect (Fig. 4 b). The critical role of Scrib in ecPlxnB1-induced cell migration was confirmed with an independent siRNA in both MIA PaCa-2 cells (Fig. S4, a and b) and in T3M4 cells (Fig. S4, c and d). To verify the interaction between Scrib and Sema4A, we performed coimmunoprecipitation experiments in HEK293T cells. Although we could not detect an interaction of the intracellular portion of Sema4A with Scrib in the absence of ecPlxnB1, we observed binding in the presence of ecPlxnB1 (Fig. 4 c). These results were confirmed in MIA PaCa-2, T3M4, and CaD2 cells, which express endogenous Scrib (Fig. 4 d). Furthermore, in primary BMDCs, application of ecPlxnB1 resulted in the formation of a Sema4A–Scrib complex (Fig. 4 e). In addition to Scrib, our GST-pulldown approach (Fig. 4 a) had identified seven other potential Sema4A-interacting proteins, the siRNA-mediated knockdown of four of which showed an inhibition of the ecPlxnB1-induced promigratory effect (Fig. 4 b). However, in coimmunoprecipitation experiments in the absence and presence of ecPlxnB1, we could not detect an interaction between Sema4A and these proteins (encoded by the *snx27*, *tln1*, *prkd2*, or *ran* genes; not depicted). To map the interaction sites between Scrib and Sema4A, we cloned several deletion mutants of Scrib (Fig. 4 f) and tested for their ability to interact with the intracellular portion of Sema4A in HEK293T cells. This analysis showed that Scrib binds to the intracellular portion of Sema4A via its C-terminal part (amino acids 1224 and 1630), a region to which no functions have been assigned so far (Fig. 4 g).

Sema4A reverse signaling regulates the activity of small GTPases

Scrib has been shown to control the activity of the small GTPases Rac1 and Cdc42, which are crucially involved in the regulation of cell migration (Audebert et al., 2004; Osmani et al., 2006; Momboisse et al., 2009; Spiering and Hodgson, 2011). We therefore tested whether Plexin-B1 regulates Cdc42 and/or Rac1 activity through Sema4A and Scrib. We found that application of ecPlxnB1 to MIA PaCa-2 or T3M4 cells resulted in a reduction of Cdc42 and Rac1 activity (Fig. 5, a and b; and Fig. S5, a–c). Furthermore, exposure to ecPlxnB1 also lowered the activity of Cdc42 in BMDCs (Fig. 5 c). The inhibition of Cdc42 and Rac1 activity by ecPlxnB1 was dependent on Sema4A, as shRNA-mediated knockdown of Sema4A in MIA PaCa-2 cells (Figs. 5 a and S5, a and b) or knockout of Sema4A in BMDCs (Fig. 5 c) rendered cells unresponsive to ecPlxnB1. The loss of the ecPlxnB1-induced effect on Cdc42 and Rac1 activity in MIA PaCa-2 cells with shRNA-mediated knockdown of Sema4A could be fully rescued by overexpression of shRNA-resistant wild-type Sema4A, but not overexpression of Sema4AΔC (Figs. 5 a and S5, a and b). Of note, the effect of ecPlxnB1 on the activity of small GTPases was restricted to Cdc42 and Rac1, as activities of the closely related small GTPases RhoA, RhoB, or RhoC were not influenced (Fig. S5, d–f). To gain further insight into the ecPlxnB1-induced Sema4A-mediated modulation of Cdc42 and Rac1 activity, we tried to visualize Cdc42 and Rac1 activity with spatial and temporal resolution. Along these lines, we used Förster resonance energy transfer (FRET) assays using Cdc42 and Rac1 biosensors (Martin et al., 2016) in different experimental setups. In a first series of measurements, we applied ecPlxnB1 to the medium so that the plasma membrane of each analyzed cell got uniformly exposed to ecPlxnB1. In full accordance with the pulldown assays, this led to a reduction of Cdc42 and Rac1 activity in a Sema4A-

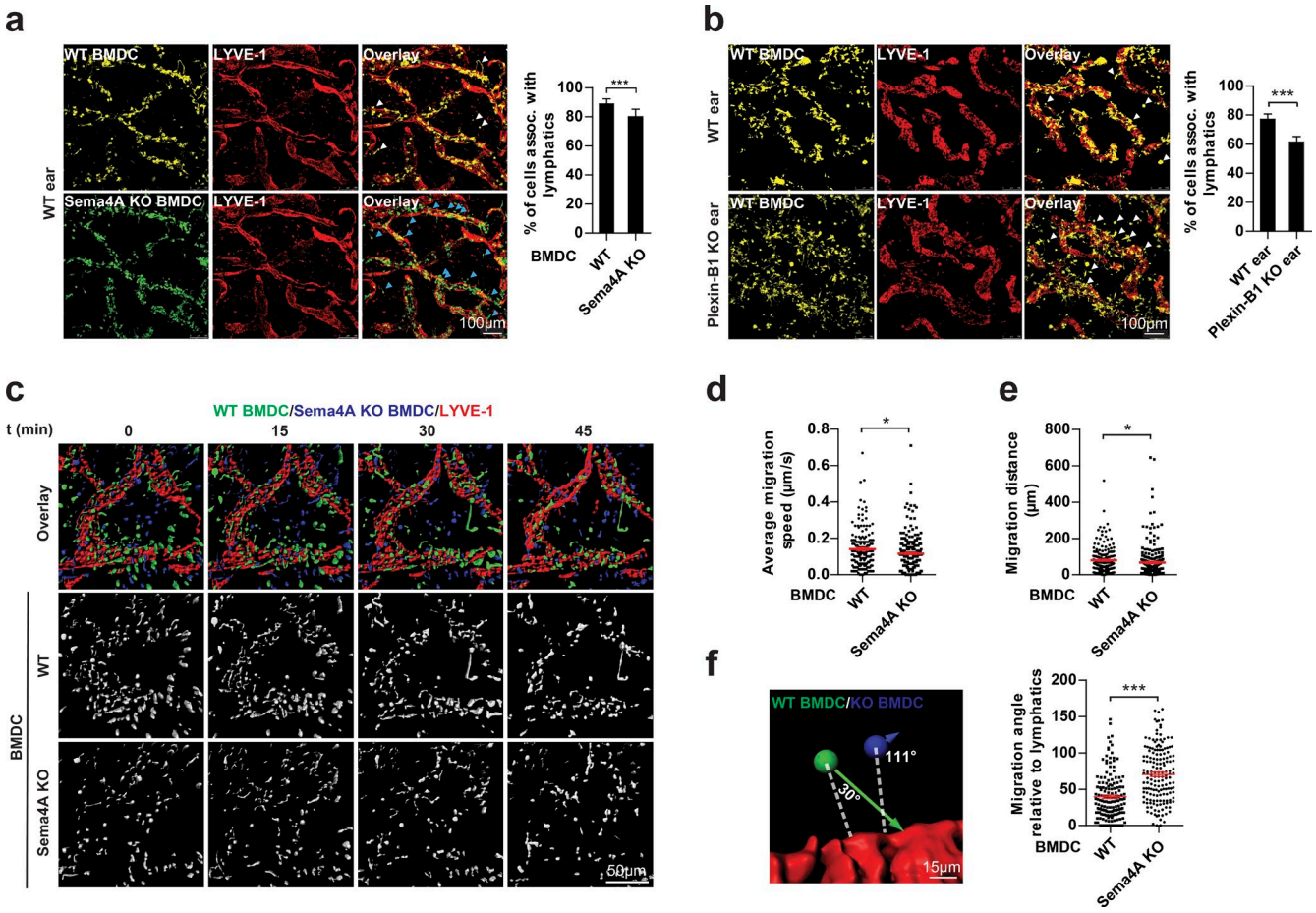

Figure 3. **Plexin-B1 and Sema4A regulate DC migration ex vivo.** (a) Mature BMDCs generated from wild-type (WT) and Sema4A knockout mice (Sema4A KO) were fluorescently labeled (WT, yellow; Sema4A KO, green), mixed 1:1, and used for the ex vivo migration assay (right). After 1.5 h, BMDCs associated with lymphatic vessels were quantified (left). Examples of wild-type (white arrows) and Sema4A-knockout (blue arrows) BMDCs not associated with lymphatic vessels are marked. (b) Mature BMDCs generated from wild-type mice were allowed to migrate into ear sheets of wild-type or Plexin-B1 knockout mice for 1.5 h (right). BMDCs associated with lymphatic vessels were quantified (left). Examples of BMDCs not associated with lymphatic vessels are marked with white arrows. (c) Mature BMDCs generated from wild-type and Sema4A knockout mice were fluorescently labeled (WT, green; Sema4A KO, blue), mixed 1:1, and used for live-cell imaging (different time points shown). (d and e) Quantification of migration speed (d) and distance (e) of BMDCs with the indicated genotypes. (f) Analysis of the migration angle of BMDCs relative to the lymphatic vessel. Dashed white lines represent the shortest possible distance to lymphatic vessels. Red horizontal lines indicate means ± SEM. Colored arrows represent vectors of BMDC migration. Bar graphs in a and b show mean values ± SD from three independent experiments. Graphs in d–f are based on six independent experiments. Total numbers of analyzed cells are WT, n = 1,993 and Sema4A KO, n = 1,785 (a); WT ear, n = 1,786 and Plexin-B1 KO ear, n = 1,560 (b); WT, n = 172 and Sema4A KO, n = 239 (d and e); and WT, n = 157 and Sema4A KO, n = 164 (f). Error bars represent means ± SD (a and b) or SEM (d–f). *, P < 0.05; ***, P < 0.001.

dependent manner (Fig. 5, d and e; and Fig. S5 g). However, in our in vitro and ex vivo migration assays, and likely also under physiological conditions in vivo, the concentration of Plexin-B1 is not uniform around the cell, but rather it forms a gradient. In an attempt to mimic a physiologically relevant situation, we therefore exposed cells to a polarized ecPlxnB1 stimulus. We observed that Cdc42 activity decreased at the site of ecPlxnB1 application (Fig. 5 f), indicating that a gradient of ecPlxnB1 translates into polarized modulation of Cdc42 activity. To test whether ecPlxnB1 regulates Cdc42 and Rac1 activity through Sema4A/Scrib, we aimed at specifically interfering with the Sema4A–Scrib interaction. We hypothesized that overexpression of the C-terminal portion of Scrib (amino acids 1224–1630), which interacts with Sema4A (see Identification of downstream effectors of Sema4A), could compete for the interaction of wild-type Scrib with Sema4A, thereby acting as a dominant-negative form. Indeed, we found that overexpression of the C-terminal portion of Scrib decreased the ecPlxnB1-induced interaction of Sema4A and Scrib and blocked ecPlxnB1-induced Rac1 deactivation (Figs. 5 g and S5 h).

Plexin-B1 regulates Scrib localization through Sema4A

Scrib localization critically influences Scrib activity (Navarro et al., 2005; Osmani et al., 2006). We therefore tested whether Sema4A could regulate the distribution of Scrib within cells. Although Scrib localized to the plasma membrane of T3M4 cells in the absence of ecPlxnB1 (Fig. 6 a), application of ecPlxnB1 induced the internalization of Scrib in a time-dependent manner (Fig. 6, a and b, top left panel). This effect of ecPlxnB1 was dependent on Sema4A, as shRNA-mediated knockdown of Sema4A (Fig. S5 i) restored the plasma membrane localization of Scrib (Fig. 6 b). Expression of shRNA-resistant wild-type Sema4A in Sema4A shRNA–expressing cells rendered the cells responsive to ecPlxnB1 again, whereas expression of shRNA-resistant mutant Sema4AΔC did not (Fig. 6 b). These

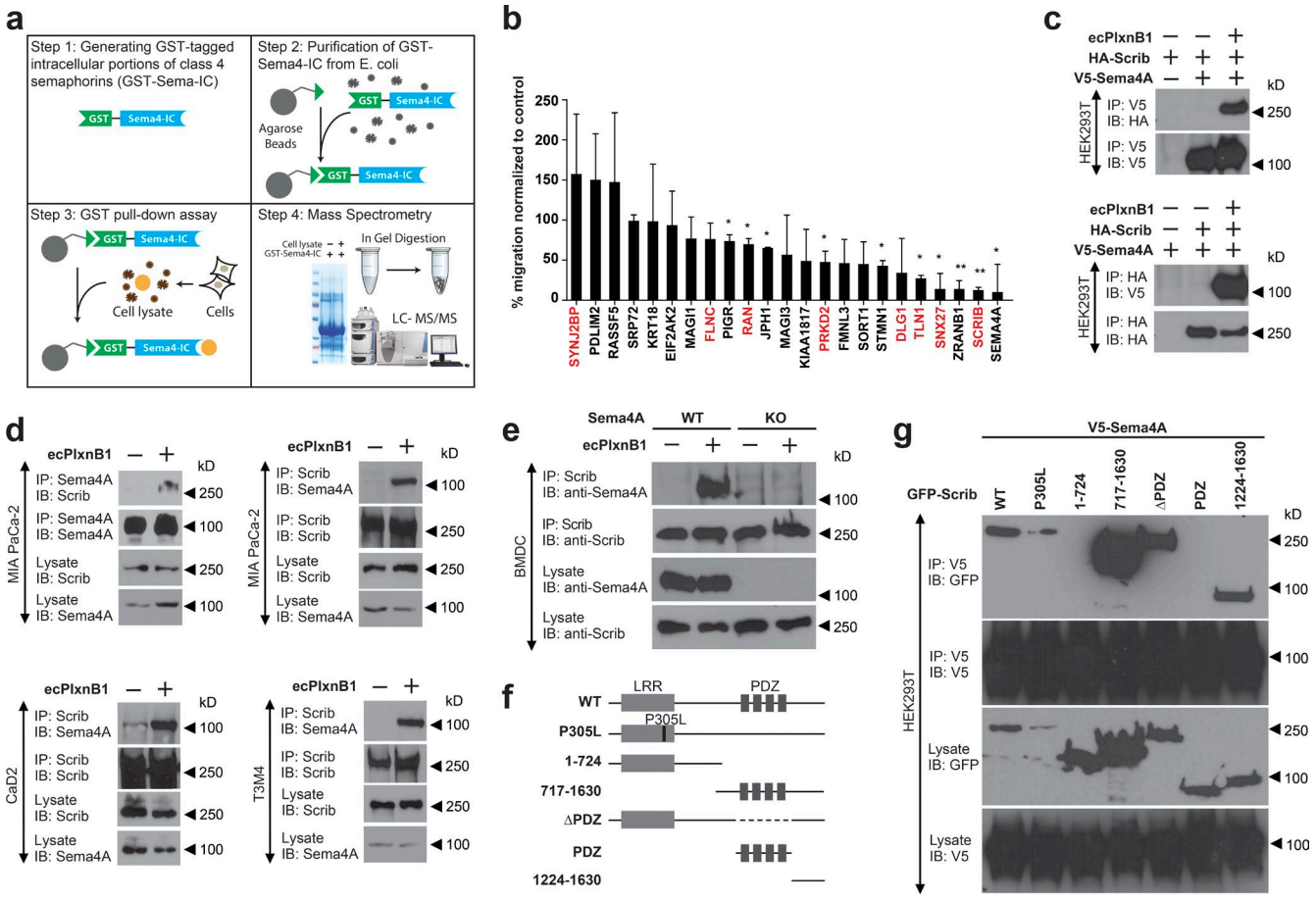

Figure 4. **Scrib mediates reverse signaling of Sema4A.** (a) Workflow for the identification of proteins interacting with the intracellular portion (IC) of class 4 semaphorins by mass spectrometry. For details, see Materials and methods. (b) MIA PaCa-2 cells transfected with the indicated siRNAs were examined in transwell migration assays in the absence or presence of 150 nM ecPlxnB1. The ecPlxnB1-induced effect on cells transfected with siRNA directed against the gene of interest is normalized to the ecPlxnB1-induced effect on cells transfected with control siRNA (percentage). Genes encoding for proteins identified as potential Sema4A-interacting partners by the GST pulldown approach are colored in red. Error bars represent the mean ± SD. (c) HEK293T cells were transfected with plasmids encoding HA-tagged Scrib (HA-Scrib) alone or together with V5-tagged Sema4A (V5-Sema4A). After serum starvation and stimulation with or without ecPlxnB1, cells were lysed, and proteins were immunoprecipitated (IP) using anti-V5 or anti-HA antibodies coupled to protein A/G sepharose. Bound proteins were then separated and visualized using anti-HA or anti-V5 antibodies (as indicated). (d) MIA PaCa-2, CaD2, or T3M4 cells were serum starved and stimulated as indicated. Sema4A or Scrib were immunoprecipitated using the respective antibodies (IP). Protein complexes were visualized by Western blotting (immunblotting [IB]). (e) Mature BMDCs were generated from wild-type mice (WT) or Sema4A knockout mice (Sema4A KO). Cells were stimulated with or without 150 nM ecPlxnB1 and lysed, and protein complexes were immunoprecipitated using anti Scrib antibodies. Proteins were then immunoblotted using specific antibodies as indicated. (f) Schematic representation of GFP-tagged Scrib constructs used in this study. (g) HEK293T cells were transfected with V5-tagged Sema4A and constructs encoding GFP-tagged wild-type or deletion mutants of Scrib (as indicated). Protein complexes were immunoprecipitated in the presence of 150 nM ecPlxnB1 using anti-V5 antibody and visualized using the indicated antibodies. Error bars represent means ± SD. *, $P < 0.05$.

results indicate that Plexin-B1 regulates Scrib localization through Sema4A reverse signaling. Given that Scrib has been shown to be involved in the regulation of protein trafficking (Lahuna et al., 2005), we next asked whether Scrib, in turn, controls the localization of Sema4A. After application of ecPlxnB1, we detected a significant decrease of Sema4A surface expression (Fig. 6 c). This effect was abrogated by siRNA-mediated knockdown of Scrib (Fig. 6 c).

Plexin-B1–Sema4A reverse signaling interferes with the interaction of Scrib and βPIX

Scrib has been shown to regulate Rac1 and Cdc42 activity through its interaction with the Rac1/Cdc42 guanine nucleotide exchange factor (GEF) βPIX (Audebert et al., 2004; Osmani et al., 2006; Nola et al., 2008). Therefore, we tested whether Plexin-B1, through its receptor Sema4A, could impact the Scrib–βPIX complex. In HEK293T cells, application of ecPlxnB1 reduced the binding of Scrib to βPIX (Fig. 7 a). To test for the functional significance of the Scrib–βPIX interaction in the Plexin-B1–Sema4A reverse signaling pathway, we performed siRNA-mediated knockdown of βPIX in MIA PaCa-2 cells. We observed that βPIX silencing abolished the effects of ecPlxnB1 on cell migration (Fig. 7 b). In THP1 cells differentiated to DCs, which endogenously express Sema4A (Fig. S4 e), ecPlxnB1 led to the deactivation of Cdc42 and increased cell migration in a Scrib- and βPIX-dependent manner (Fig. 7, c and d; and Fig. S4 f). Cells with siRNA-mediated knockdown of Scrib or βPIX were still partially responsive to the known promigratory factors FBS or CCL19 (Fig. 7, b and d; Berges et al., 2005; Marsland et al., 2005), indicating a specific role for Scrib and βPIX in the Plexin-B1–Sema4A reverse signaling

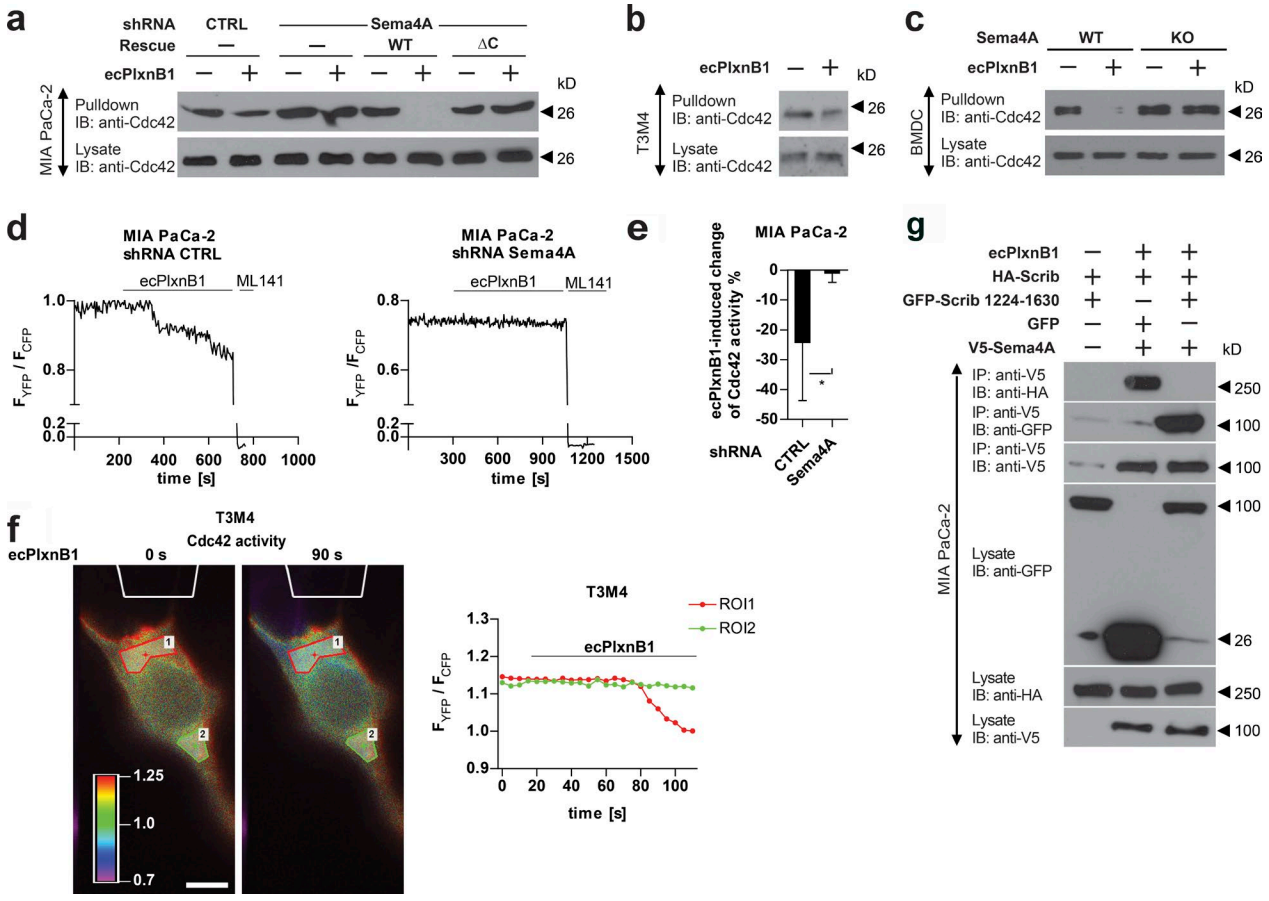

Figure 5. **Sema4A reverse signaling regulates the activity of Rac1 and Cdc42.** (a) MIA PaCa-2 cells stably expressing control shRNA or Sema4A shRNA either alone or together with shRNA-resistant wild-type (WT) or mutated (ΔC) Sema4A (as indicated) were starved and stimulated with or without 150 nM ecPlxnB1, and active Cdc42 was precipitated as described in Materials and methods. (b) T3M4 cells were treated with or without 150 nM ecPlxnB1, and Cdc42 activity was measured (pulldown). (c) Mature BMDCs generated from wild-type or Sema4A knockout mice (Sema4A KO) were stimulated with or without 150 nM ecPlxnB1 for 20 min. Cells were then lysed and the activity of Cdc42 was analyzed (pulldown). (d and e) MIA PaCa-2 cells stably expressing control or Sema4A shRNA were transfected with a FRET biosensor for Cdc42 and FRET ratios in response to 150 nM ecPlxnB1, and 100 µM of the Cdc42 inhibitor ML141 were analyzed as described in Materials and methods. (d) Representative traces are shown. CTRL, control. (e) The ecPlxnB1-induced change of Cdc42 activity was calculated as a percentage of the difference between the FRET ratio at baseline (before treatments) and the FRET ratio after ML141 treatment. n = 12 for control shRNA, n = 8 for Sema4A shRNA. (f) ecPlxnB1 was applied to one side of a T3M4 cell through a micropipette (as outlined in white at the top of the images) as described in Materials and methods. Shown are representative images and the corresponding FRET ratios within two different areas of the cell over time. The regions of interest (ROIs) indicate regions proximal or distal to the site of ecPlxnB1 application, respectively. Bar, 10 µm. (g) MIA PaCa-2 cells were transfected with constructs encoding HA-Scrib, V5-Sema5A, and the GFP-tagged C-terminal portion of Scrib (GFP-Scrib amino acids 1224–1630) as indicated. Cells were stimulated with or without 150 nM ecPlxnB1. Proteins interacting with Sema4A were immunoprecipitated using V5 antibody and visualized using respective antibodies. IB, immunoblotting; IP, immunoprecipitation. Error bars represent means ± SD. *, $P < 0.05$.

pathway. Moreover, blocking the Sema4A–Scrib interaction by overexpressing the C-terminal portion of Scrib (amino acids 1224–1630) in MIA PaCa-2 cells inhibited the promigratory effect of ecPlxnB1 (Fig. 7 e).

Discussion

Class 4 semaphorins are a widely expressed group of transmembrane proteins (Yazdani and Terman, 2006; Gu and Giraudo, 2013; Kang and Kumanogoh, 2013). Although the role and importance of these semaphorins as ligands have been well established (Gu and Giraudo, 2013; Roney et al., 2013; Worzfeld and Offermanns, 2014), their potential function as receptors to mediate cellular effects through reverse signaling is poorly understood (Battistini and Tamagnone, 2016). In this study, we systematically characterized a potential receptor function of a particular semaphorin, Sema4A, and analyzed cell behavior and changes in signaling pathways induced by a soluble extracellular portion of Plexin-B1. Indeed, we found that Plexin-B1 increases the migration of cancer and of DCs through reverse signaling mediated by Sema4A.

Plexin-B1 is known to bind to both Sema4A and Sema4D (Granziero et al., 2003; Yukawa et al., 2010). However, our data show that Plexin-B1 can trigger cellular effects through reverse signaling of Sema4A, but not of Sema4D. This may be explained by the existence of additional, not yet identified coreceptors or by semaphorin-specific downstream mediators.

In this study, we used a soluble extracellular portion of Plexin-B1 to activate Sema4A-mediated reverse signaling. In contrast to full-length plexins, the role and function of their secreted versions remain largely unexplored. In the case of Plexin-B1, the secreted ectodomain may be the result of alternative splicing or of proteolytic cleavage of the full-length

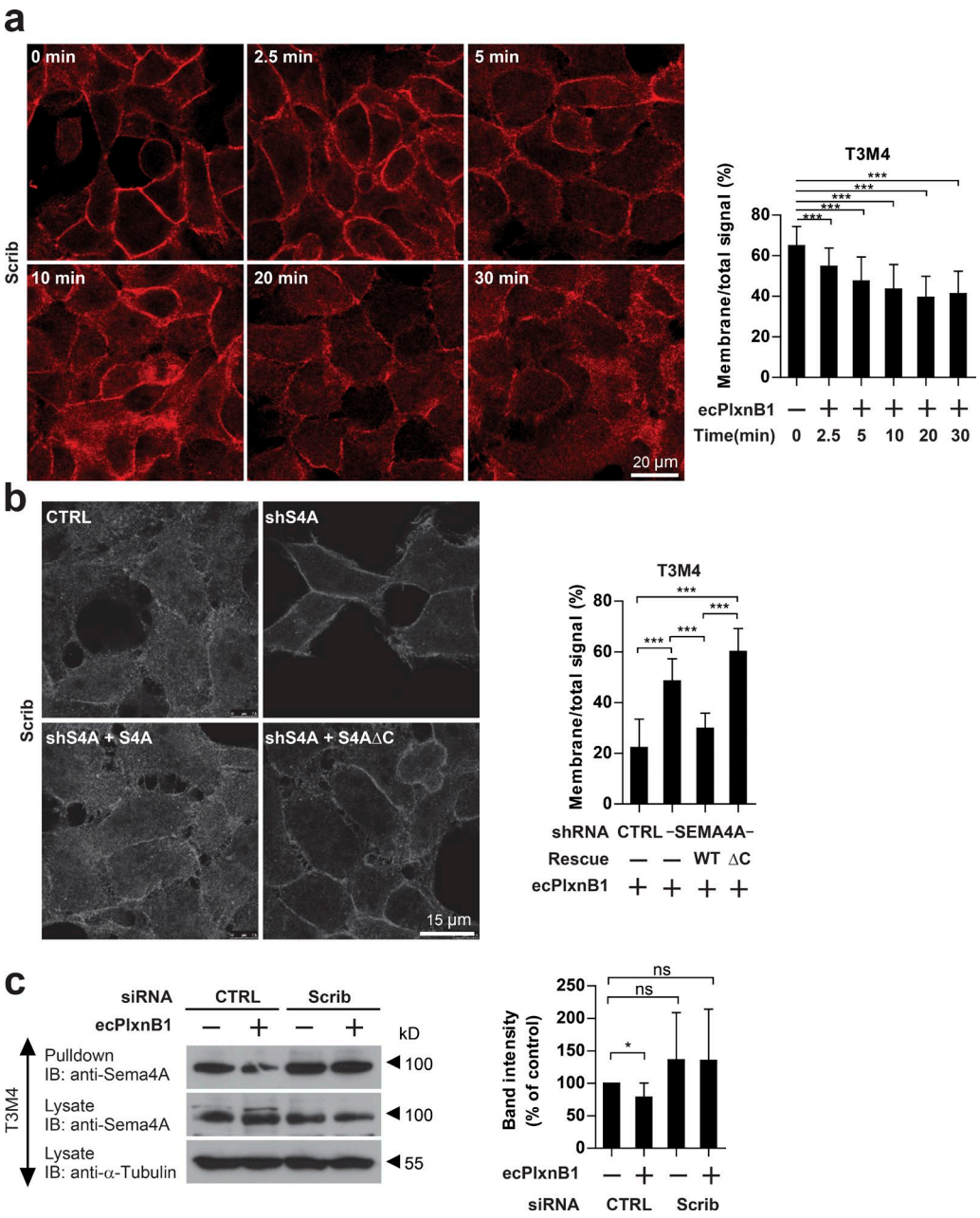

Figure 6. **Plexin-B1–Sema4A signaling induces internalization of Scrib.** (a) T3M4 cells were incubated with or without 150 nM ecPlxnB1, and Scrib was visualized by immunostaining at the indicated time points after application of ecPlxnB1. Scrib localization was analyzed using ImageJ as described in Materials and methods. Time point 0 min: $n = 41$; 2.5 min: $n = 61$; 5 min: $n = 54$; 10 min: $n = 53$; 20 min: $n = 26$; 30 min: $n = 45$. (b) T3M4 cells stably transfected with control shRNA or with Sema4A shRNA alone or together with either shRNA-resistant wild-type Sema4A (S4A) or an shRNA-resistant Sema4A intracellular deletion mutant (S4AΔC) were incubated with 150 nM ecPlxnB1 for 30 min, and Scrib was visualized by immunostaining. Scrib localization was analyzed using ImageJ as described in Materials and methods. Bar graphs show mean values ± SD from at least 10 cells per condition. (c) Surface proteins of T3M4 cells transfected with control or Scrib were biotinylated. Cells were then incubated with or without 150 nM ecPlxnB1 for 30 min, surface proteins were precipitated using streptavidin agarose, and bound Sema4A was visualized by Western blotting using an anti-Sema4A antibody (pulldown; right). Band intensities were quantified from six independent Western blots (left). ns, not significant. CTRL, control; IB, immunoblotting. Error bars represent means ± SD. *, $P < 0.05$; ***, $P < 0.001$.

protein from the cell membrane (Tamagnone et al., 1999; Artigiani et al., 2003; Ito et al., 2014). Recently, increased levels of a soluble, circulating Plexin-B1 portion were found in postmenopausal women with low bone mass (Anastasilakis et al., 2015); a secreted extracellular part of Plexin-B1 was also detected in proteomics studies (Farrah et al., 2011). Moreover, we detected soluble forms of Plexin-B1 of ∼70 kD in size released from lymphatic endothelial cells (HMVECs). This form closely resembles an alternatively spliced, secreted form of Plexin-B1 (Tamagnone et al., 1999), suggesting a physiological relevance of secreted Plexin-B1.

Migration is the key feature of DCs during their life cycle (Randolph et al., 2008; Heuzé et al., 2013; Russo et al., 2013; Teijeira et al., 2014). To home to lymph nodes, peripheral DCs must migrate toward, and enter, lymphatic vessels. The interaction between DCs and the lymphatic endothelium can be

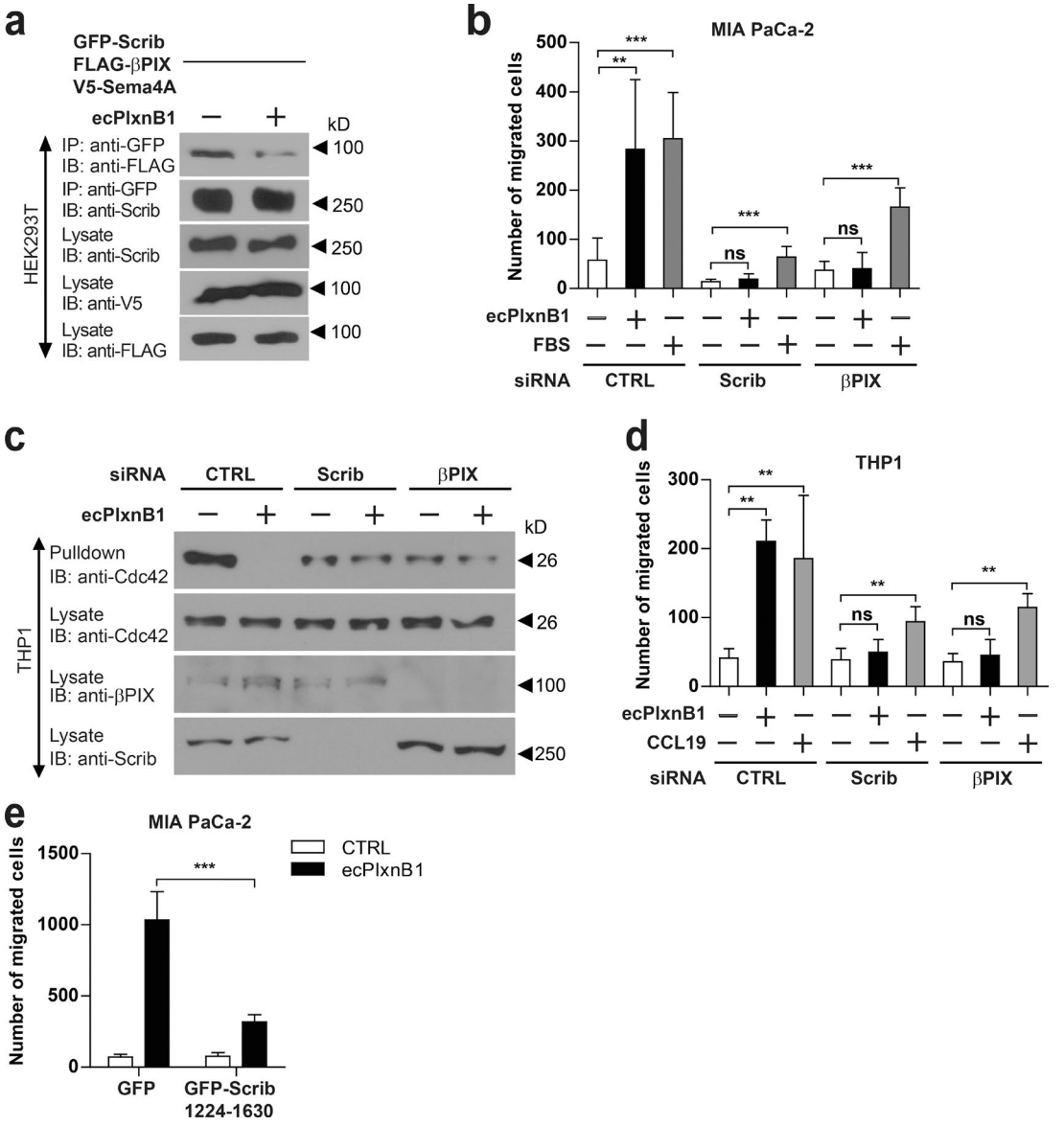

Figure 7. **Scrib and βPIX are required for Plexin-B1–Sema4A reverse signaling.** (a) HEK293T cells transfected with V5-Sema4A, GFP-Scrib, and FLAG-βPIX were stimulated with or without 150 nM ecPlxnB1. Protein complexes were precipitated using anti-GFP antibodies and visualized with immunoblotting (IB). IP, immunoprecipitation. (b) MIA PaCa-2 cells were transfected with siRNAs as indicated, and cell migration in response to 150 nM ecPlxnB1 or 10% FBS in a transwell system was analyzed as described in Materials and methods (total $n = 6$ per condition). (c and d) THP1 cells were fully differentiated to DCs as described in Materials and methods. Cells were then stimulated with 150 nM ecPlxnB1 or 25 ng/ml CCL19 (as indicated), and Cdc42 activity (c) and cell migration (d) was analyzed by using a transwell system as described in Materials and methods (total $n = 6$ per condition). ns, not significant. CTRL, control. (e) MIA PaCa-2 cells were transfected with cDNAs encoding GFP or GFP-Scrib (amino acids 1224–1630), and cell migration in response to ecPlxnB1 was measured as described in Materials and methods. Shown are mean values ± SD from three independent experiments (total $n = 8$ per condition). Error bars represent means ± SD. **, $P < 0.01$; ***, $P < 0.001$.

mediated by various molecules including ICAM1, JAM1, or CCR7 (Randolph et al., 2005), and it seems very likely that the complete set of molecules regulating the entry of DCs into lymphatic vessels is still to be determined. Our data strongly suggest that Plexin-B1 is a novel factor secreted by lymphatic endothelial cells, which regulates the migration of DCs into lymphatic vessels through Sema4A reverse signaling.

Using an unbiased approach to screen for Sema4A-interacting proteins, we identified Scrib as a binding partner for Sema4A, which is critical for the promigratory effect of Plexin-B1. This is in line with the known function of Scrib in directed cell migration and wound healing in vitro and in vivo (Dow et al., 2007; Michaelis et al., 2013). Scrib interacts with the Cdc42/Rac1 GEF, βPIX, and this interaction positively regulates the GEF activity of βPIX (Audebert et al., 2004; Osmani et al., 2006; Goicoechea et al., 2014). We tested whether Plexin-B1, through its receptor Sema4A, may influence the Scrib–βPIX interaction and, in this way, affect the ability of βPIX to activate Cdc42 and Rac1. Indeed, we observed that in cells stimulated with Plexin-B1, the Scrib–βPIX interaction was impaired, thus providing a mechanistic basis for the Plexin-B1–induced, Sema4A-mediated deactivation of Cdc42 and Rac1. Cdc42 and Rac1 are central regulators of cell migration, and numerous reports have shown that global inhibition of Cdc42 or

Rac1 activity in the cell—by expression of dominant-negative mutants, RNAi-mediated knockdown, or gene knockouts—inhibits cell migration (Ridley, 2015). It is therefore an intriguing finding of our study that the lowering of Cdc42 and Rac1 activity by Plexin-B1–Sema4A signaling correlates with a promigratory effect toward higher Plexin-B1 concentrations. Importantly, directed cell migration requires a tight spatiotemporal coordination of Rho-GTPase activities (Raftopoulou and Hall, 2004). Although their activation is necessary to promote cell movement through the formation of filopodia and lamellipodia, they need to be rapidly deactivated to ensure fluent cell movement (Sadok and Marshall, 2014). Dynamic measurements of small GTPase activity show that during cell migration, small GTPases are constantly activated and deactivated, rather than being active for the whole time (Žárský and Potocký, 2010; Gloerich and Bos, 2011; Kiyokawa et al., 2011; Tolias et al., 2011; Lawson and Burridge, 2014; Zegers and Friedl, 2014). Using FRET assays, we visualized Cdc42 activity in cells with spatial and temporal resolution and observed that Cdc42 activity decreased at the site of Plexin-B1 application, indicating that in contrast to a global inhibition of Cdc42 activity, exposure to a gradient of Plexin-B1 translates into polarized modulation of Cdc42 activity. Another interesting observation of our FRET studies was the timeline of the inhibition of Cdc42 and Rac1 activity by Plexin-B1. Although changes in Cdc42 or Rac1 activity measured by FRET typically occur within seconds after the application of a stimulus (e.g., a chemokine or growth factor; Hanna et al., 2014; Martin et al., 2016), changes of Cdc42 and Rac1 activity in response to Plexin-B1 were not detectable before 1.5–2 min. Our data therefore suggest that the promigratory effect of Plexin-B1–Sema4A signaling results from a complex spatiotemporal regulation of Cdc42 and Rac1 activity.

Importantly, the function of Scrib critically depends on its localization at the plasma membrane. Mislocalization of Scrib promotes the invasion of cells through the extracellular matrix (Dow et al., 2007, 2008). We found that the interaction of Scrib with Sema4A upon Plexin-B1 binding promotes the internalization of Scrib. Given that Scrib has several functions in addition to modulating Cdc42 and Rac1 activity through βPIX (Elsum et al., 2012), this Plexin-B1–induced internalization of Scrib is likely to contribute to the effect on cell migration. Of note, our findings are consistent with previously published data, which show that the interaction between Scrib and CD74 results in the phosphorylation of the C-terminal portion of Scrib and in the translocation of Scrib from the sites of cell-to-cell contacts at the plasma membrane to the cytoplasm, thereby effectively enhancing cancer cell migration and invasiveness (Metodieva et al., 2013).

In summary, we demonstrate that Plexin-B1–Sema4A signaling works bidirectionally. We have identified a novel signaling mechanism in which Sema4A serves as a receptor and mediates signals from its ligand Plexin-B1 to regulate migration and invasion of cancer cells as well as chemotaxis of DCs. We propose a model in which the binding of Plexin-B1 to Sema4A promotes the interaction of Sema4A with Scrib, resulting in a destabilization of the Scrib–βPIX complex and internalization of Scrib, thereby lowering the Cdc42/Rac1 GEF activity of βPIX and decreasing Cdc42 and Rac1 activity. The tight spatiotemporal integration of these events then controls directed cell migration. Reverse signaling might be a common feature of transmembrane semaphorins, turning the semaphorin–plexin system into a bidirectional, rather than unidirectional, communication system between cells to regulate various biological processes.

Materials and methods

Cell culture and transfection

MDA-MB-231 and Calu-3 were purchased from ATCC; CaD2, A431, and SK-OV-3 were purchased from Cell Line Service. MIA PaCa-2, CFPAC, AsPc, and T3M4 were gifts from N. Giese, and SHSY-5Y cells were provided by S. Rieken (University Hospital Heidelberg, Bergheim, Germany). HeLa were provided by M. Bähr (German Cancer Research Center, Heidelberg, Germany). HMVEC-dLyAd cells and human umbilical vein endothelial cells were purchased from Lonza and cultured using the manufacturer's instructions. MIA PaCa-2, A431, MDA-MB-231, Calu-3, SHSY-5Y, CFPAC, HeLa, and HEK293T cell lines were maintained in DMEM supplemented with 10% FBS. T3M4 and AsPc cell lines were maintained in RPMI-1640 supplemented with 10% FBS. SK-OV-3 cells were maintained in McCoy's 5a supplemented with 10% FBS. THP1 cells were provided by B. Strilic (Max Planck Institute for Heart and Lung Research, Bad Nauheim, Germany). Cells were maintained in RPMI-1640 supplemented with 10% FBS and L-glutamine. To differentiate maturate THP1 cells into dendritic lineage cells, recombinant human IL-4 (100 ng/ml = 1,500 IU/ml; AF-200-04; PeproTech) and granulocyte–macrophage colony-stimulating factor (GM-CSF; 100 ng/ml = 2,000 IU/ml; 315-03; PeproTech) were added to the cell culture medium for 5 d. To maturate the DCs from THP1 cells, recombinant human TNF (20 ng/ml = 2,000 IU/ml; 300-01A; PeproTech) and 200 ng/ml ionomycin (I24222; Thermo Fisher Scientific) were added to the cell culture medium. Cells were then incubated for 1–3 d in a humidified incubator and then used for experiments. siRNA transfections of THP1 were performed using the Amaxa Cell Line Nucleofector kit V (Lonza) before cell maturation. All cells were maintained at 37°C and 5% CO_2. cDNA transfection in HEK293T cells was performed by the calcium phosphate method (Swiercz et al., 2002). Cells were transfected with cDNA by using Lipofectamine 2000 (Thermo Fisher Scientific) according to the manufacturer's instructions. RNAiMAX reagent (Thermo Fisher Scientific) was used for the siRNA transfection.

Stably transfected MIA PaCa-2 and T3M4 cells were generated using lentiviruses according to the manufacturer's protocols (Sigma-Aldrich). Cells were selected in 1 µg/ml puromycin. For rescue experiments with Sema4A constructs, GFP-positive cells were sorted with a JSAN cell sorter (Bay Bioscience Co., Ltd.).

Antibodies and reagents

The following antibodies were purchased from commercial sources: anti-GFP (1: 2,000; ChromoTek), rabbit polyclonal anti-Sema4A (1:500; C1C3; GeneTex), anti-Scrib (1:1,000; 4475; Cell Signaling Technology), anti-RhoA (1:400; clone 67B9; Cell Signaling Technology), anti-RhoB (1:500; 2098S; Cell Signaling Technology), anti-RhoC (1:500; 3430S; Cell Signaling Technology), anti-Scrib (1:1,000; sc-28737; Santa Cruz Biotechnology, Inc.), mouse monoclonal anti–α-tubulin (1:1,000; clone DM1A; Sigma-Aldrich), anti-HA (Roche), anti–HA-HRP (Sigma-Aldrich), anti–MYC-HRP (Sigma-Aldrich), anti–FLAG-HRP (Sigma-Aldrich), anti-Rac1 (1:500; 05–389; clone 23A8; EMD Millipore), anti-V5 (1:1,000; AbD Serotec), anti-Cdc42 (1:1,000; BD), rat monoclonal anti–LYVE-1 (1:500; clone 223322; R&D Systems), rabbit polyclonal anti-βPIX (1:400; 4515; Cell Signaling Technology), hamster monoclonal anti–CD11c-phycoerythrin (PE; 1:100; 12-0114-81; eBioscience), anti–B220-FITC (1:100; 553088; BD), anti–mouse T cell receptor (TCR)–PerCP/Cy5.5 (1:100; clone H57-597; BioLegend), Fc-blocking antibody (1:100; clone 2.4G2; Bio X Cell), rabbit anti–goat Cy3 (1:200; Jackson ImmunoResearch Laboratories, Inc.), goat polyclonal anti–Plexin-B1 (1:400; AF3749; R&D Systems), and anti-Sema4D (1:1,000; 610670; BD).

The rabbit polyclonal anti-Sema4A antibody 1–1-1-B1 was generated by ABmart against the peptide C-RTSASDVDADNN.GM-CSF and used at a 1:1,000 dilution. TNF (PeproTech) was used at concentrations of 20 ng/ml and 10 ng/ml. CCL19 (R&D Systems) was used at a final concentration of 25 ng/ml.

Plasmids and cloning

cDNA clones of human Sema4A were purchased from GE Healthcare. N-terminally V5-tagged full-length Sema4A and its deletion mutant Sema4AΔC (amino acids 1–707) were generated by PCR and subcloned into pcDNA3.1. A secreted Myc-His–tagged form of Plexin-B1 (ecPlxnB1; amino acids 20–534) in the pSecTag2 vector was described previously (Worzfeld et al., 2012). For lentivirus production, V5-tagged Sema4A or Sema4AΔC was inserted into pLVX-IRES-ZsGreen1 vector or pLVX-IRES-mCherry vector. pSPAX and pMD2G vectors were from Sigma-Aldrich. The intracellular parts of human Sema4A (amino acids 705–761), Sema4B (amino acids 734–832), Sema4C (amino acids 685–833), Sema4D (amino acids 756–862), Sema4F (amino acids 681–770), and Sema4G (amino acids 697–838) were cloned into pGEX4T-1 vector. Identities of all clones were confirmed by sequencing. HA-tagged Scrib and GFP-tagged Scrib constructs were described previously (Audebert et al., 2004). FLAG-tagged βPIX was described previously (Osmani et al., 2006; Dacquin et al., 2011).

Mice

Sema4A knockout ES clones (ID: EPD0105_3_B05) were purchased from EUCOMM and microinjected into C57BL/6 blastocysts. To generate constitutive Sema4A knockout mice, mice carrying the Sema4A "knockout-first" allele were crossed with E2a-Cre mice. The successful knockout of Sema4A was confirmed by Southern blotting. B6.Cg-Tg(Itgax-Venus)1Mnz/J expressing YFP under the CD11c promoter were purchased from The Jackson Laboratory. To generate mice lacking Sema4A and expressing YFP in CD11c-positive cells, Sema4A knockout mice were crossed with mice expressing YFP under the control of the CD11c (Itgax) promotor. Plexin-B1 knockout mice were generated as described previously (Deng et al., 2007). Mice were maintained under specific pathogen-free conditions. All procedures involving animals were performed in accordance with German Animal Welfare legislation.

Complete list of siRNA/shRNA and primers used

siRNAs targeting human SEMA4A (SI04368567), SEMA4B (SI04283209), SEMA4C (SI04354056, SI04362197), SEMA4D (SI03053701, SI04952332), SEMA4F (SI04163019, SI04170726), SEMA4G (SI04188198, SI04230303), SNX27 (SI04209772, SI04220755), DLG1 (SI03046099, SI03102799), SYNJ2BP (SI04243848, SI04315535), RAN (SI04950505, SI04950512), FLNC (SI03648820, SI03648813), TLN1 (SI00301931, SI00086982), SCRIB (SI04182290, SI04295655), SORT1 (SI00729316, SI03115168), MAGI3 (SI02660448, SI02644439), ZRANB1 (SI00118860, SI00118867), EIF2AK2 (SI02223011, SI02223018), MAGI1 (SI04234328, SI03181080), JPH1 (SI04289887, SI04294829), PDLIM2 (SI00681625, SI04957029), KRT18 (SI02653658, SI03187996), PIGR (SI00040887, SI02629151), RASSF5 (SI03056816, SI03058895), STMN1 (SI05389986, SI00301875), PRKD2 (SI02224768, SI02224775), FMNL3 (SI04149607, SI04188884), SRP72 (SI04334981, SI04361308), and KIAA1817 (SI00460887, SI00460894) were purchased from QIAGEN. siRNA targeting human βPIX (SASI_Hs02_00325961, SASI_Hs02_00325962) was purchased from Sigma-Aldrich. A second independent Scrib siRNA was purchased from QIAGEN (SI05053041).

shRNA targeting human Sema4A (TRCN0000058137) was from Sigma-Aldrich. The following RT-PCR primers were synthetized by Sigma-Aldrich: human SEMA4A (5′-GCTGCCCTTCAACGTCAT-3′, 5′-AGGTGAAGACTGCGTAGATGTG-3′), human SEMA4B (5′-TGTGGCCTCAGCCTACATT-3′, 5′-GATCTTGTCATCATCGCCTTG-3′), human SEMA4C (5′-GAAGAAGGGCACCAACTTCA-3′, 5′-TGGCTCCATCAAGTCCTGTA-3′), human SEMA4D (5′-CTTCCTGAAAGCCCGACTC-3′, 5′-GCAGCACATTGAAGACCAAG-3′), human SEMA4F (5′-TCCTGAAGATGAGCGGTTG-3′, 5′-AGGAAGGGTGGTGAGAATCC-3′), human SEMA4G (5′-AGTGCAGTGGGTGATGATGA-3′, 5′-TGAGTGAAGCTGCCAGAGC-3′), human GAPDH (5′-GCATCCTGGGCTACACTGA-3′, 5′-CCAGCGTCAAAGGTGGAG-3′), human SCRIB (5′-CTCTGCCACATTCCTCACC-3′, 5′-GGGGTGGCAGTGGTTATG-3′), and mouse SEMA4A (5′-ATGGAGTCTCCTGCGTGTTT-3′, 5′-GAAGCAGGTGGCAGTGATG-3′); (5′-CCCAGCCTGTTCTCAAGACT-3′, 5′-ATAGACGACCTGGGTGGATG-3′); (5′-GCAGCTGCCATTCAACATC-3′, 5′-CACAGACTGCTGAGCTCCTG-3′); (5′-AACCCGGAGTGGGTATGC-3′, 5′-TTGGGGACTGTCAGGACTTC-3′).

RT-PCR

RNA was extracted using the RNeasy Mini kit (QIAGEN). cDNA was synthesized by reverse transcription (First Strand cDNA Synthesis kit; Roche). 60 ng cDNA per reaction was used. Primers were designed with the online tool provided by Roche. Quantitative PCR was performed using the Light-Cycler 480 Probes Master system from Roche.

Protein purification

ecPlxnB1 (amino acids 20–534 of human Plexin-B1) was purified from conditioned medium of transiently transfected HEK293 cells (Worzfeld et al., 2012), whereas His-tagged Sema4D was produced from supernatants of stably transfected CHO cells (Love et al., 2003) using metal-ion affinity chromatography (HisPUR Cobalt Resin; Thermo Fisher Scientific) followed by gel filtration chromatography (Superdex S200 HR10/30; GE Healthcare). GST fusion proteins were expressed in *Escherichia coli* (DE3 Rosetta; EMD Millipore) and purified using Protino Agarose 4B (Macherey and Nagel; Swiercz et al., 2002).

Binding of ecPlxnB1 to Sema4A-expressing cells

MIA PaCa-2 cells were exposed to 150 nM ecPlxnB1 for 20 min, washed three times with PBS, and incubated with an anti–Myc-HRP antibody. After washing three times with PBS, HRP activity was measured using the General Elisa Protocol (Dako).

Proliferation assay

For proliferation assays, cells were seeded onto 6-well plates and counted using a Neubauer chamber on four consecutive days.

GST pulldown assay

3×10^7 cells (MIA PaCa-2, HEK293T, CaD2, or SK-OV-3 cell lines) were lysed in radioimmunoprecipitation assay (RIPA) lysis buffer (150 mM NaCl, 50 mM Tris, pH 7.4, 1% Triton X-100, 0.1% sodium dodecyl sulfate, 0.25% sodium deoxycholate, 1 µg/ml each of leupeptin, aprotinin, and pepstatin, and 1 mM 4-(2-aminoethyl)-benzosulfonylfluoridhydrochloride). GST fusion proteins (consisting of GST and the intracellular portions of different class 4 semaphorins) bound to Protino Agarose 4B were incubated with these lysates at 4°C for 2 h. Purified GST fusion proteins incubated with lysis buffer (without cells) and purified GST alone (lacking semaphorin intracellular portions) incubated with cell lysates or lysis buffer served as controls. Protino Agarose 4B beads were then washed three times in RIPA lysis buffer, and bound proteins were eluted by boiling with Laemmli buffer.

Mass spectrometry analysis

Identification of proteins bound to the intracellular portions of class 4 semaphorins (see previous paragraph) was performed in the Biomolecular Mass Spectrometry Facility of the Max Planck Institute for Heart and Lung Research. Peptides were measured on an LTQ-Oribtrap XL instrument (Thermo Fisher Scientific). An Agilent 1200 (Agilent Technologies) was coupled via a nanoelectrospray ionization source to the mass spectrometer. A binary buffer system was used: (A) 0.5% acetic acid in H_2O and (B) 0.5% acetic acid in 80% acetonitrile. 15-cm in-house–packed columns were used for peptide separation along an increasing buffer B content concentration from 5 to 39% within 50 min followed by a washing step with 95% buffer B and a reequilibration to 5% buffer B. The mass spectrometer operated in a Top5 method, and collision-induced dissociation fragmentation (normal collision energy: 35) was used for peptide identification.

MaxQuant (version 1.2.0.18; Max Planck Institute of Biochemistry) and the implemented Andromeda search engine was used to correlate measured mass spectrometry (MS)/MS spectra with the *Homo sapiens* or *Mus musculus* International Protein Index database. The false discovery rate on peptide and protein level was set to 1%, and the minimal peptide length was seven amino acids. MS and MS/MS mass tolerance were kept as default settings. N-terminal protein acetylation and oxidation at methionine residues were defined as variable modifications, whereas carbamidomethylation at cysteine residues was set as a fixed modification. Ratios to identify possible binding partners of semaphorins were calculated based on the label-free quantification intensity of protein groups.

Using a scoring system based on several parameters (label-free quantification intensity, number of identified peptides, number of identified unique peptides, and number of cell lines in which a potential interaction partner was identified), we identified a total of 65 potential interaction partners for class 4 semaphorins. Of those, we excluded 10 proteins with known nuclear localization and function (e.g., histones), leaving 55 candidates. The 22 candidates with the highest score in the scoring system were further tested in migration assays using siRNAs directed against these candidates (see next section).

Migration and invasion assays

For transwell migration assays, 5×10^4 cells were serum starved overnight and seeded into 96-transwell migration plates (order MAM IC8S10; EMD Millipore). Control buffer or buffer containing 150 nM ecPlxnB1 was added to the lower chamber of the respective wells. 18 h later, nonmigrated cells on the upper surface of the filter were removed, and migrated cells on the lower surface of the filter were fixed in methanol and stained with toluidine blue. Cell migration was analyzed by measuring the staining intensity using ImageJ (National Institutes of Health; labeling of y axis in the respective experiments with "cell migration") or by counting the number of migrated cells manually (labeling of y axis in the respective experiments with "number of migrated cells"). For transwell migration assays of THP1 cells, cells were allowed to migrate for 3 h, and cells in the lower chamber were counted.

For 3D migration assays of DCs, 10^7 cells/ml mature BMDCs, 10^7 cells/ml $CD11c^+$ splenic DCs (purity > 80%), or 10^7 cells/ml THP1 cells were mixed with a collagen I gel and put into µ-Slide Chemotaxis^{3D} migration chambers (ibidi). 150 nM ecPlxnB1 was added to one of the reservoirs, and cell migration was imaged by live-cell imaging over a period of 2–4 h by capturing images every 1–2 min (see Microscope image acquisition). Cells were tracked using the Manual Tracking Plug-in (Fiji) of ImageJ. For every 3D migration experiment, the tracks of 10–37 cells were monitored. The y-forward migration index (FMI_y) and center of mass were calculated using the Chemotaxis and Migration tool plugin (ibidi) for ImageJ. The FMI_y represents the efficiency of the forward migration of cells in relation to the y axis, and the center of mass represents the averaged point of all cell endpoints (ibidi).

Invasion assays were performed as described previously (Worzfeld et al., 2012).

DC isolation, culture, and transfection

For the isolation of splenic DCs, spleens from C57BL/6 mice were digested by collagenase D and passed through a 40-µm nylon mesh to remove debris. Erythrocytes were lysed and cells were washed three times with RPMI-1640 medium. $CD11c^+$ DCs were FACS sorted with CD11c-PE antibody. For the generation of BMDCs, bone marrow was flushed from C57BL/6 mice femurs and tibias with ice-cold RPMI-1640 medium. Erythrocytes were lysed and cells were passed through a 40-µm nylon mesh to remove debris. Cells were washed three times with RPMI-1640 medium and put into 100-mm Petri dishes in complete growth medium plus 20 ng/ml GM-CSF (Inaba et al., 1992). Medium was changed every 2 or 3 d, and DCs were collected from days 6 to 8. 10 ng/ml TNF was added overnight to DCs for maturation. BMDCs were transfected using lentiviruses carrying V5-tagged Sema4A-IRES-mCherry or V5-tagged Sema4AΔC-IRES-ZsGreen1. In brief, HEK293 cells were transiently transfected with vectors for generating lentiviruses. 3 d after transfection, the virus-containing medium was collected and filtered. 10 µg/ml hexadimethrine bromide (Polybrene) and 20 mM Hepes were added to viruses. BMDCs were prepared as described in this paragraph and seeded onto 24-well plates. The next day (day 2), virus-containing medium was added, and the plates were centrifuged at 2,500 rpm at 30°C for 90 min. The plates were incubated at 37°C and 5% CO_2 for 3 h followed by centrifugation at 1,500 rpm for 5 min. Supernatant was removed and fresh culture medium was added to the cells. The procedure was repeated two more times (on days 3 and 4; Dudziak et al., 2007).

FACS sorting

MIA PaCa-2 and T3M4 cells infected with pLVX-IRES-ZsGreen1-Sema4A or pLVX-IRES-ZsGreen1-Sema4AΔC lentiviruses were trypsinized, and cells were resuspended in PBS containing 0.5% BSA and 1 mM EDTA. GFP-positive cells were sorted using a JSAN cell sorter. Splenic DCs were labeled and sorted with CD11c-PE. Purity was determined using FACS Canto II (BD) by labeling the cells with CD11c-PE, B220-FITC, and TCR-Cy5.5.

Ex vivo crawl-in assay

The ex vivo crawl-in assay was adapted from Weber and Sixt (2013). C57BL/6 mice were sacrificed, their ears removed, and ears were separated into dorsal and ventral sheets. Ventral ear sheets without cartilage were immunostained and mounted on self-made migration chambers with the dermal surface exposed on top. DCs were labeled with 1.25 µm seminaphtharhodafluor (Thermo Fisher Scientific) or 1.25 µm carboxyfluorescein succinimidyl ester (Thermo Fisher Scientific) in culture medium and added on top of the dermis. After 5–10 min of incubation at 37°C and 5% CO_2, noninfiltrated DCs were removed, and new medium was added on top of the dermis. Ear sheets were incubated in a climatized (37°C, 5% CO_2) chamber for different time periods, washed with PBS, fixed in 1% PFA, and mounted for confocal microscopy using Fluoromount W (Serva Electrophoresis). Alternatively, migration of DCs was recorded by live-cell imaging.

Immunoprecipitations and Cdc42/Rac1 pulldown assays

For protein immunoprecipitation, cells were lysed in ice-cold RIPA buffer (150 mM NaCl, 50 mM Tris, pH 7.4, 1% Triton X-100, 0.1% sodium dodecyl sulfate, 0.25% sodium deoxycholate, 1 µg/ml each of leupeptin, aprotinin, and pepstatin, 1 mM 4-(2-aminoethyl)-benzosulfonylfluoridhydrochloride, and 1 mM Na_3VO_4). Lysates were

centrifuged, and supernatants were incubated with different antibodies in the presence of Protein A/G PLUS Agarose (Santa Cruz Biotechnology, Inc.). Agarose beads were then centrifuged and washed several times using ice-cold RIPA buffer. Finally, antibody-bound proteins were eluted by boiling the beads in Laemmli buffer. Samples were then subjected to Western blotting.

Activities of Rac1 and Cdc42 were measured using GST-tagged PAK1 (Swiercz et al., 2002). The activities of RhoA, RhoB, and RhoC were tested using GST-tagged Rhotekin (Ren and Schwartz, 2000).

Western blot

Western blotting was performed according to standard laboratory protocols. In brief, cell lysates or precipitates were separated using SDS-PAGE, followed by transfer onto nitrocellulose membranes and blocking of nonspecific binding sites with 5% nonfat milk in Tris-buffered saline with Tween 20 (TBST) for 1 h at room temperature. The blots were probed with primary antibodies at 4°C overnight, washed three times with TBST, incubated with secondary antibodies for 1.5 h at room temperature, and washed again three times with TBST, and proteins were visualized using an ECL system (Thermo Fisher Scientific). Western blot band intensities were quantified using the Gel Analysis tool of ImageJ.

Cell surface biotinylation and precipitation of biotinylated proteins

Cell surface biotinylation was performed using the EZ-Link Sulfo-NHS-Biotinylation kit (Thermo Fisher Scientific) according to the manufacturer's instructions. Biotinylated cells were lysed in ice-cold RIPA buffer (Fig. S1 f) or a buffer containing 25 mM Tris-HCl, pH 7.4, 150 mM NaCl, 5 mM EDTA, and 1% Triton X-100 (Fig. 6 c), and biotinylated surface proteins were precipitated from the clarified lysates using streptavidin agarose (Thermo Fisher Scientific).

Immunostaining and imaging

Cells were starved overnight and stimulated with 150 nM Plexin-B1. Cells were then fixed with 4% PFA and stained using an anti-Scrib (1:300; sc-28737) and an Alexa Fluor 594–conjugated secondary antibody. Images were acquired using an SP5 confocal microscope (Leica Biosystems). Membrane staining versus total staining was analyzed using the Profile Plot function of ImageJ.

Microarray analysis

Expression data from lymphatic endothelial cells were analyzed based on Affymetrix Mouse Genome 430 2.0 arrays, downloaded from GEO (dataset GSE22034; four replicates). The array signals were aggregated and normalized via robust multiarray average, including quantile normalization, and were used to calculate the frequency distribution of gene expressions. In total, 45,101 single gene expression values were used. To generate one single representative value for each gene, the mean of all replicates was calculated. The resulting values were used for frequency calculation. Bin size was set to 0.5.

FRET measurements

Plasmids encoding Cdc42 (pTriEx4-Cdc42-2G) and Rac1 (pTriEx4-Rac1-2G) FRET biosensors were a gift from O. Pertz (University of Bern, Bern, Switzerland; plasmids 66110 and 68814, respectively; Addgene; Fritz et al., 2015). MIA PaCa-2 or T3M4 cells were transfected with plasmids encoding a FRET biosensor and MeGAP (=SRGAP3) and seeded on glass coverslips. For FRET measurements, cells were incubated in FRET buffer (137 mM NaCl, 5.4 mM KCl, 2 mM $CaCl_2$, 1 mM $MgCl_2$, and 10 mM Hepes, pH 7.3). FRET imaging was performed on an inverted fluorescence microscope (Eclipse T*i*; Nikon) as described previously (Wolters et al., 2015) using a light-emitting diode excitation system (pE-2; CoolLED) containing light-emitting diodes emitting light at 425 nm and 500 nm, respectively. Dual emission (cyan and yellow) images with an exposure time of 2 ms were acquired with a rate of 12/min. Ratio images (F535/F480) were calculated without correction for bleedthrough and false excitation. Cells that were not responsive to the Cdc42 inhibitor, ML141, or to the Rac inhibitor, EHT1864, were excluded from the analysis.

Experiments designed to measure the effects of a local Plexin-B1 stimulus were performed by placing a micropipette on one side of the cell while the cell was exposed to a continuous laminar flow of FRET buffer from the opposite direction that was applied using a perfusion system (ALA-VC3-8SP; ALA Scientific Instruments). Images were acquired every 5 s with illumination times of 40–60 ms. Because FRET was measured with a monomolecular sensor, no background subtraction and bleedthrough corrections were performed. The images were generated using NIS Elements (Nikon) and show averages of four consecutive data points to reduce noise.

Microscope image acquisition

Live-cell imaging of DC migration in vitro was performed with an inverse microscope (37°C, 5% CO_2, 10× objective; IX-1; Olympus). Confocal laser-scanning microscopes used in this study were Leica Biosystems SP5 (40× and 63× objectives) and Leica Biosystems SP8 (for live-cell imaging; 37°C, 5% CO_2, 20× objective). Analysis of live-cell imaging of DC migration ex vivo was done by Imaris software.

Statistical analysis

Statistical significance was evaluated by Student's *t* test. Data shown in Figs. 1 (b–f), 2 (a–d), 3 (a and b), 4 (b), 5 (d), 6 (a–c), 7 (b, d, and e), S1 (a, g, h, j, and k), S2 (b, d, and e), S3 (a), S4 (b, d, and f), and S5 (a and g) are means ± SD. Data shown in Fig. 3 (d–f) are means ± SEM. *, $P < 0.05$; **, $P < 0.01$; ***, $P < 0.001$.

Online supplemental material

Fig. S1 provides additional evidence that the extracellular portion of Plexin-B1 increases cancer cell migration through Sema4A. Fig. S2 shows the purity of FACS-sorted splenic DCs, the generation and validation of Sema4A-deficient mice, and the migration parameters of DCs in response to different stimuli. Fig. S3 depicts additional analyses of BMDC migration toward ear lymphatic vessels and provides an expression analysis of lymphatic endothelial cells and BMDCs. Fig. S4 shows that the promigratory effect of the extracellular portion of Plexin-B1 depends on Scrib. Fig. S5 demonstrates the modulation of Rho-GTPase activities by the extracellular portion of Plexin-B1 through Sema4A–Scrib. Video 1 shows the migration of wild-type and Sema4A-deficient BMDCs toward ear lymphatic vessels ex vivo.

Acknowledgments

The authors would like to acknowledge Svea Hümmer and Justin Mirus for secretarial help with the preparation of the manuscript and Dagmar Magalei for technical help.

T. Worzfeld is supported by grants from the German Research Foundation (grants WO 1901/2-1 and GRK 2213) and from the University Medical Center Giessen and Marburg. J.M. Swiercz and T. Sun were supported by the German Research Foundation (grant SW 148/1-1). J.-P. Borg's laboratory is supported by La Ligue Nationale Contre le Cancer (Label Ligue JPB) and Site de Recherche Intégrée sur le Cancer (INCa-DGOS-Inserm 6038). J.-P. Borg is a scholar of Institut Universitaire de France. T. Worzfeld, J.M. Swiercz, and S. Offermanns hold a patent on B-type plexin antagonists and uses thereof.

The authors declare no additional competing financial interests.

Submitted: 1 February 2016
Revised: 30 September 2016
Accepted: 13 November 2016

References

Anastasilakis, A.D., S.A. Polyzos, P. Makras, A. Gkiomisi, G. Sakellariou, M. Savvidis, A. Papatheodorou, P. Kokkoris, and E. Terpos. 2015. Circulating semaphorin-4D and plexin-B1 levels in postmenopausal women with low bone mass: the 3-month effect of zoledronic acid, denosumab or teriparatide treatment. *Expert Opin. Ther. Targets.* 19:299–306. http://dx.doi.org/10.1517/14728222.2014.983078

Andermatt, I., N.H. Wilson, T. Bergmann, O. Mauti, M. Gesemann, S. Sockanathan, and E.T. Stoeckli. 2014. Semaphorin 6B acts as a receptor in post-crossing commissural axon guidance. *Development.* 141:3709–3720. http://dx.doi.org/10.1242/dev.112185

Armendáriz, B.G., A. Bribian, E. Pérez-Martínez, A. Martínez, F. de Castro, E. Soriano, and F. Burgaya. 2012. Expression of Semaphorin 4F in neurons and brain oligodendrocytes and the regulation of oligodendrocyte precursor migration in the optic nerve. *Mol. Cell. Neurosci.* 49:54–67. http://dx.doi.org/10.1016/j.mcn.2011.09.003

Artigiani, S., D. Barberis, P. Fazzari, P. Longati, P. Angelini, J.W. van de Loo, P.M. Comoglio, and L. Tamagnone. 2003. Functional regulation of semaphorin receptors by proprotein convertases. *J. Biol. Chem.* 278:10094–10101. http://dx.doi.org/10.1074/jbc.M210156200

Audebert, S., C. Navarro, C. Nourry, S. Chasserot-Golaz, P. Lécine, Y. Bellaiche, J.L. Dupont, R.T. Premont, C. Sempéré, J.M. Strub, et al. 2004. Mammalian Scribble forms a tight complex with the βPIX exchange factor. *Curr. Biol.* 14:987–995. http://dx.doi.org/10.1016/j.cub.2004.05.051

Basile, J.R., T. Afkhami, and J.S. Gutkind. 2005. Semaphorin 4D/plexin-B1 induces endothelial cell migration through the activation of PYK2, Src, and the phosphatidylinositol 3-kinase-Akt pathway. *Mol. Cell. Biol.* 25:6889–6898. http://dx.doi.org/10.1128/MCB.25.16.6889-6898.2005

Battistini, C., and L. Tamagnone. 2016. Transmembrane semaphorins, forward and reverse signaling: have a look both ways. *L. Cell. Mol. Life Sci.* 73:1609–1622.

Berges, C., C. Naujokat, S. Tinapp, H. Wieczorek, A. Höh, M. Sadeghi, G. Opelz, and V. Daniel. 2005. A cell line model for the differentiation of human dendritic cells. *Biochem. Biophys. Res. Commun.* 333:896–907. http://dx.doi.org/10.1016/j.bbrc.2005.05.171

Burkhardt, C., M. Müller, A. Badde, C.C. Garner, E.D. Gundelfinger, and A.W. Püschel. 2005. Semaphorin 4B interacts with the post-synaptic density protein PSD-95/SAP90 and is recruited to synapses through a C-terminal PDZ-binding motif. *FEBS Lett.* 579:3821–3828. http://dx.doi.org/10.1016/j.febslet.2005.05.079

Cafferty, P., L. Yu, H. Long, and Y. Rao. 2006. Semaphorin-1a functions as a guidance receptor in the *Drosophila* visual system. *J. Neurosci.* 26:3999–4003. http://dx.doi.org/10.1523/JNEUROSCI.3845-05.2006

Casazza, A., P. Fazzari, and L. Tamagnone. 2007. Semaphorin signals in cell adhesion and cell migration: functional role and molecular mechanisms. *Adv. Exp. Med. Biol.* 600:90–108. http://dx.doi.org/10.1007/978-0-387-70956-7_8

Dacquin, R., C. Domenget, A. Kumanogoh, H. Kikutani, P. Jurdic, and I. Machuca-Gayet. 2011. Control of bone resorption by semaphorin 4D is dependent on ovarian function. *PLoS One.* 6. http://dx.doi.org/10.1371/journal.pone.0026627

Deng, S., A. Hirschberg, T. Worzfeld, J.Y. Penachioni, A. Korostylev, J.M. Swiercz, P. Vodrazka, O. Mauti, E.T. Stoeckli, L. Tamagnone, et al. 2007. Plexin-B2, but not Plexin-B1, critically modulates neuronal migration and patterning of the developing nervous system *in vivo*. *J. Neurosci.* 27:6333–6347. http://dx.doi.org/10.1523/JNEUROSCI.5381-06.2007

Dow, L.E., J.S. Kauffman, J. Caddy, K. Zarbalis, A.S. Peterson, S.M. Jane, S.M. Russell, and P.O. Humbert. 2007. The tumour-suppressor Scribble dictates cell polarity during directed epithelial migration: regulation of Rho GTPase recruitment to the leading edge. *Oncogene.* 26:2272–2282. http://dx.doi.org/10.1038/sj.onc.1210016

Dow, L.E., I.A. Elsum, C.L. King, K.M. Kinross, H.E. Richardson, and P.O. Humbert. 2008. Loss of human Scribble cooperates with H-Ras to promote cell invasion through deregulation of MAPK signalling. *Oncogene.* 27:5988–6001. http://dx.doi.org/10.1038/onc.2008.219

Driessens, M.H., H. Hu, C.D. Nobes, A. Self, I. Jordens, C.S. Goodman, and A. Hall. 2001. Plexin-B semaphorin receptors interact directly with active Rac and regulate the actin cytoskeleton by activating Rho. *Curr. Biol.* 11:339–344. http://dx.doi.org/10.1016/S0960-9822(01)00092-6

Dudziak, D., A.O. Kamphorst, G.F. Heidkamp, V.R. Buchholz, C. Trumpfheller, S. Yamazaki, C. Cheong, K. Liu, H.W. Lee, C.G. Park, et al. 2007. Differential antigen processing by dendritic cell subsets in vivo. *Science.* 315:107–111. http://dx.doi.org/10.1126/science.1136080

Elsum, I., L. Yates, P.O. Humbert, and H.E. Richardson. 2012. The Scribble-Dlg-Lgl polarity module in development and cancer: from flies to man. *Essays Biochem.* 53:141–168. http://dx.doi.org/10.1042/bse0530141

Farrah, T., E.W. Deutsch, G.S. Omenn, D.S. Campbell, Z. Sun, J.A. Bletz, P. Mallick, J.E. Katz, J. Malmstrom, R. Ossola, et al. 2011. A high-confidence human plasma proteome reference set with estimated concentrations in PeptideAtlas. *Mol. Cell. Proteomics.* 10. http://dx.doi.org/10.1074/mcp.M110.006353

Fong, K.P., C. Barry, A.N. Tran, E.A. Traxler, K.M. Wannemacher, H.Y. Tang, K.D. Speicher, I.A. Blair, D.W. Speicher, T. Grosser, and L.F. Brass. 2011. Deciphering the human platelet sheddome. *Blood.* 117:e15–e26. http://dx.doi.org/10.1182/blood-2010-05-283838

Fritz, R.D., D. Menshykau, K. Martin, A. Reimann, V. Pontelli, and O. Pertz. 2015. SrGAP2-dependent integration of membrane geometry and Slit-Robo-repulsive cues regulates fibroblast contact inhibition of locomotion. *Dev. Cell.* 35:78–92. http://dx.doi.org/10.1016/j.devcel.2015.09.002

Giusti, B., G. Fibbi, F. Margheri, S. Serratì, L. Rossi, F. Poggi, I. Lapini, A. Magi, A. Del Rosso, M. Cinelli, et al. 2006. A model of anti-angiogenesis: differential transcriptosome profiling of microvascular endothelial cells from diffuse systemic sclerosis patients. *Arthritis Res. Ther.* 8. http://dx.doi.org/10.1186/ar2002

Gloerich, M., and J.L. Bos. 2011. Regulating Rap small G-proteins in time and space. *Trends Cell Biol.* 21:615–623. http://dx.doi.org/10.1016/j.tcb.2011.07.001

Godenschwege, T.A., H. Hu, X. Shan-Crofts, C.S. Goodman, and R.K. Murphey. 2002. Bi-directional signaling by Semaphorin 1a during central synapse formation in *Drosophila*. *Nat. Neurosci.* 5:1294–1301. http://dx.doi.org/10.1038/nn976

Goicoechea, S.M., S. Awadia, and R. Garcia-Mata. 2014. I'm coming to GEF you: Regulation of RhoGEFs during cell migration. *Cell Adhes. Migr.* 8:535–549. http://dx.doi.org/10.4161/cam.28721

Granziero, L., P. Circosta, C. Scielzo, E. Frisaldi, S. Stella, M. Geuna, S. Giordano, P. Ghia, and F. Caligaris-Cappio. 2003. CD100/Plexin-B1 interactions sustain proliferation and survival of normal and leukemic $CD5^+$ B lymphocytes. *Blood.* 101:1962–1969. http://dx.doi.org/10.1182/blood-2002-05-1339

Gu, C., and E. Giraudo. 2013. The role of semaphorins and their receptors in vascular development and cancer. *Exp. Cell Res.* 319:1306–1316. http://dx.doi.org/10.1016/j.yexcr.2013.02.003

Gurrapu, S., and L. Tamagnone. 2016. Transmembrane semaphorins: multimodal signaling cues in development and cancer. *Cell Adhes. Migr.* 10:675–691. http://dx.doi.org/10.1007/978-0-387-70956-7_8

Hanna, S., V. Miskolci, D. Cox, and L. Hodgson. 2014. A new genetically encoded single-chain biosensor for Cdc42 based on FRET, useful for live-cell imaging. *PLoS One.* 9. http://dx.doi.org/10.1371/journal.pone.0096469

Hemming, M.L., J.E. Elias, S.P. Gygi, and D.J. Selkoe. 2009. Identification of β-secretase (BACE1) substrates using quantitative proteomics. *PLoS One.* 4. http://dx.doi.org/10.1371/journal.pone.0008477

Heuzé, M.L., P. Vargas, M. Chabaud, M. Le Berre, Y.J. Liu, O. Collin, P. Solanes, R. Voituriez, M. Piel, and A.M. Lennon-Duménil. 2013. Migration of dendritic cells: physical principles, molecular mechanisms, and functional implications. *Immunol. Rev.* 256:240–254. http://dx.doi.org/10.1111/imr.12108

Hota, P.K., and M. Buck. 2012. Plexin structures are coming: opportunities for multilevel investigations of semaphorin guidance receptors, their cell signaling mechanisms, and functions. *Cell. Mol. Life Sci.* 69:3765–3805. http://dx.doi.org/10.1007/s00018-012-1019-0

Inaba, K., M. Inaba, N. Romani, H. Aya, M. Deguchi, S. Ikehara, S. Muramatsu, and R.M. Steinman. 1992. Generation of large numbers of dendritic cells from mouse bone marrow cultures supplemented with granulocyte/macrophage colony-stimulating factor. *J. Exp. Med.* 176:1693–1702. http://dx.doi.org/10.1084/jem.176.6.1693

Inagaki, S., Y. Ohoka, H. Sugimoto, S. Fujioka, M. Amazaki, H. Kurinami, N. Miyazaki, M. Tohyama, and T. Furuyama. 2001. Sema4c, a transmembrane semaphorin, interacts with a post-synaptic density protein, PSD-95. *J. Biol. Chem.* 276:9174–9181. http://dx.doi.org/10.1074/jbc.M009051200

Ito, T., T. Bai, T. Tanaka, K. Yoshida, T. Ueyama, M. Miyajima, T. Negishi, T. Kawasaki, H. Takamatsu, H. Kikutani, et al. 2014. Estrogen-dependent proteolytic cleavage of semaphorin 4D and plexin-B1 enhances semaphorin 4D-induced apoptosis during postnatal vaginal remodeling in pubescent mice. *PLoS One.* 9. http://dx.doi.org/10.1371/journal.pone.0097909

Janssen, B.J., R.A. Robinson, F. Pérez-Brangulí, C.H. Bell, K.J. Mitchell, C. Siebold, and E.Y. Jones. 2010. Structural basis of semaphorin–plexin signalling. *Nature.* 467:1118–1122. http://dx.doi.org/10.1038/nature09468

Jongbloets, B.C., and R.J. Pasterkamp. 2014. Semaphorin signalling during development. *Development.* 141:3292–3297. http://dx.doi.org/10.1242/dev.105544

Kang, S., and A. Kumanogoh. 2013. Semaphorins in bone development, homeostasis, and disease. *Semin. Cell Dev. Biol.* 24:163–171. http://dx.doi.org/10.1016/j.semcdb.2012.09.008

Kiyokawa, E., K. Aoki, T. Nakamura, and M. Matsuda. 2011. Spatiotemporal regulation of small GTPases as revealed by probes based on the principle of Förster resonance energy transfer (FRET): Implications for signaling and pharmacology. *Annu. Rev. Pharmacol. Toxicol.* 51:337–358. http://dx.doi.org/10.1146/annurev-pharmtox-010510-100234

Kolodkin, A.L., D.J. Matthes, and C.S. Goodman. 1993. The semaphorin genes encode a family of transmembrane and secreted growth cone guidance molecules. *Cell.* 75:1389–1399. http://dx.doi.org/10.1016/0092-8674(93)90625-Z

Komiyama, T., L.B. Sweeney, O. Schuldiner, K.C. Garcia, and L. Luo. 2007. Graded expression of semaphorin-1a cell-autonomously directs dendritic targeting of olfactory projection neurons. *Cell.* 128:399–410. http://dx.doi.org/10.1016/j.cell.2006.12.028

Kruger, R.P., J. Aurandt, and K.L. Guan. 2005. Semaphorins command cells to move. *Nat. Rev. Mol. Cell Biol.* 6:789–800. http://dx.doi.org/10.1038/nrm1740

Kumanogoh, A., S. Marukawa, K. Suzuki, N. Takegahara, C. Watanabe, E. Ch'ng, I. Ishida, H. Fujimura, S. Sakoda, K. Yoshida, and H. Kikutani. 2002. Class IV semaphorin Sema4A enhances T-cell activation and interacts with Tim-2. *Nature.* 419:629–633. http://dx.doi.org/10.1038/nature01037

Lahuna, O., M. Quellari, C. Achard, S. Nola, G. Méduri, C. Navarro, N. Vitale, J.P. Borg, and M. Misrahi. 2005. Thyrotropin receptor trafficking relies on the hScrib-βPIX-GIT1-ARF6 pathway. *EMBO J.* 24:1364–1374. http://dx.doi.org/10.1038/sj.emboj.7600616

Lawson, C.D., and K. Burridge. 2014. The on-off relationship of Rho and Rac during integrin-mediated adhesion and cell migration. *Small GTPases.* 5. http://dx.doi.org/10.4161/sgtp.27958

Love, C.A., K. Harlos, N. Mavaddat, S.J. Davis, D.I. Stuart, E.Y. Jones, and R.M. Esnouf. 2003. The ligand-binding face of the semaphorins revealed by the high-resolution crystal structure of SEMA4D. *Nat. Struct. Biol.* 10:843–848. http://dx.doi.org/10.1038/nsb977

Luo, Y., D. Raible, and J.A. Raper. 1993. Collapsin: a protein in brain that induces the collapse and paralysis of neuronal growth cones. *Cell.* 75:217–227. http://dx.doi.org/10.1016/0092-8674(93)80064-L

Marsland, B.J., P. Bättig, M. Bauer, C. Ruedl, U. Lässing, R.R. Beerli, K. Dietmeier, L. Ivanova, T. Pfister, L. Vogt, et al. 2005. CCL19 and CCL21 induce a potent proinflammatory differentiation program in licensed dendritic cells. *Immunity.* 22:493–505. http://dx.doi.org/10.1016/j.immuni.2005.02.010

Martin, K., A. Reimann, R.D. Fritz, H. Ryu, N.L. Jeon, and O. Pertz. 2016. Spatio-temporal co-ordination of RhoA, Rac1 and Cdc42 activation during prototypical edge protrusion and retraction dynamics. *Sci. Rep.* 6. http://dx.doi.org/10.1038/srep21901

Messina, A., and P. Giacobini. 2013. Semaphorin signaling in the development and function of the gonadotropin hormone-releasing hormone system. *Front. Endocrinol. (Lausanne).* 4.

Metodieva, G., N.C. Nogueira-de-Souza, C. Greenwood, K. Al-Janabi, L. Leng, R. Bucala, and M.V. Metodiev. 2013. CD74-dependent deregulation of the tumor suppressor scribble in human epithelial and breast cancer cells. *Neoplasia.* 15:660–668. http://dx.doi.org/10.1593/neo.13464

Michaelis, U.R., E. Chavakis, C. Kruse, B. Jungblut, D. Kaluza, K. Wandzioch, Y. Manavski, H. Heide, M.J. Santoni, M. Potente, et al. 2013. The polarity protein Scrib is essential for directed endothelial cell migration. *Circ. Res.* 112:924–934. http://dx.doi.org/10.1161/CIRCRESAHA.112.300592

Momboisse, F., E. Lonchamp, V. Calco, M. Ceridono, N. Vitale, M.F. Bader, and S. Gasman. 2009. βPIX-activated Rac1 stimulates the activation of phospholipase D, which is associated with exocytosis in neuroendocrine cells. *J. Cell Sci.* 122:798–806. http://dx.doi.org/10.1242/jcs.038109

Nagai, H., N. Sugito, H. Matsubara, Y. Tatematsu, T. Hida, Y. Sekido, M. Nagino, Y. Nimura, T. Takahashi, and H. Osada. 2007. CLCP1 interacts with semaphorin 4B and regulates motility of lung cancer cells. *Oncogene.* 26:4025–4031. http://dx.doi.org/10.1038/sj.onc.1210183

Nakatsuji, Y., T. Okuno, M. Moriya, T. Sugimoto, M. Kinoshita, H. Takamatsu, S. Nojima, T. Kimura, S. Kang, D. Ito, et al. 2012. Elevation of Sema4A implicates Th cell skewing and the efficacy of IFN-β therapy in multiple sclerosis. *J. Immunol.* 188:4858–4865. http://dx.doi.org/10.4049/jimmunol.1102023

Navarro, C., S. Nola, S. Audebert, M.J. Santoni, J.P. Arsanto, C. Ginestier, S. Marchetto, J. Jacquemier, D. Isnardon, A. Le Bivic, et al. 2005. Junctional recruitment of mammalian Scribble relies on E-cadherin engagement. *Oncogene.* 24:4330–4339. http://dx.doi.org/10.1038/sj.onc.1208632

Nelson, G.M., T.P. Padera, I. Garkavtsev, T. Shioda, and R.K. Jain. 2007. Differential gene expression of primary cultured lymphatic and blood vascular endothelial cells. *Neoplasia.* 9:1038–1045. http://dx.doi.org/10.1593/neo.07643

Nola, S., M. Sebbagh, S. Marchetto, N. Osmani, C. Nourry, S. Audebert, C. Navarro, R. Rachel, M. Montcouquiol, N. Sans, et al. 2008. Scrib regulates PAK activity during the cell migration process. *Hum. Mol. Genet.* 17:3552–3565. http://dx.doi.org/10.1093/hmg/ddn248

Ohoka, Y., M. Hirotani, H. Sugimoto, S. Fujioka, T. Furuyama, and S. Inagaki. 2001. Semaphorin 4C, a transmembrane semaphorin, [corrected] associates with a neurite-outgrowth-related protein, SFAP75. *Biochem. Biophys. Res. Commun.* 280:237–243. http://dx.doi.org/10.1006/bbrc.2000.4080

Osmani, N., N. Vitale, J.P. Borg, and S. Etienne-Manneville. 2006. Scrib controls Cdc42 localization and activity to promote cell polarization during astrocyte migration. *Curr. Biol.* 16:2395–2405. http://dx.doi.org/10.1016/j.cub.2006.10.026

Platt, A.M., and G.J. Randolph. 2013. Dendritic cell migration through the lymphatic vasculature to lymph nodes. *Adv. Immunol.* 120:51–68 http://dx.doi/org/10.1016/B978-0-12-417028-5.00002-8.

Raftopoulou, M., and A. Hall. 2004. Cell migration: Rho GTPases lead the way. *Dev. Biol.* 265:23–32. http://dx.doi.org/10.1016/j.ydbio.2003.06.003

Randolph, G.J., V. Angeli, and M.A. Swartz. 2005. Dendritic-cell trafficking to lymph nodes through lymphatic vessels. *Nat. Rev. Immunol.* 5:617–628. http://dx.doi.org/10.1038/nri1670

Randolph, G.J., J. Ochando, and S. Partida-Sánchez. 2008. Migration of dendritic cell subsets and their precursors. *Annu. Rev. Immunol.* 26:293–316. http://dx.doi.org/10.1146/annurev.immunol.26.021607.090254

Ren, X.D., and M.A. Schwartz. 2000. Determination of GTP loading on Rho. *Methods Enzymol.* 325:264–272. http://dx.doi.org/10.1016/S0076-6879(00)25448-7

Ridley, A.J. 2015. Rho GTPase signaling in cell migration. *Curr. Opin. Cell Biol.* 36:103–112. http://dx.doi.org/10.1016/j.ceb.2015.08.005

Roney, K., E. Holl, and J. Ting. 2013. Immune plexins and semaphorins: old proteins, new immune functions. *Protein Cell.* 4:17–26. http://dx.doi.org/10.1007/s13238-012-2108-4

Russo, E., M. Nitschké, and C. Halin. 2013. Dendritic cell interactions with lymphatic endothelium. *Lymphat. Res. Biol.* 11:172–182. http://dx.doi.org/10.1089/lrb.2013.0008

Sadok, A., and C.J. Marshall. 2014. Rho GTPases: masters of cell migration. *Small GTPases.* 5. http://dx.doi.org/10.4161/sgtp.29710

Spiering, D., and L. Hodgson. 2011. Dynamics of the Rho-family small GTPases in actin regulation and motility. *Cell Adhes. Migr.* 5:170–180. http://dx.doi.org/10.4161/cam.5.2.14403

Swiercz, J.M., R. Kuner, J. Behrens, and S. Offermanns. 2002. Plexin-B1 directly interacts with PDZ-RhoGEF/LARG to regulate RhoA and growth cone morphology. *Neuron.* 35:51–63. http://dx.doi.org/10.1016/S0896-6273(02)00750-X

Swiercz, J.M., T. Worzfeld, and S. Offermanns. 2008. ErbB-2 and Met reciprocally regulate cellular signaling via plexin-B1. *J. Biol. Chem.* 283:1893–1901. http://dx.doi.org/10.1074/jbc.M706822200

Takamatsu, H., and A. Kumanogoh. 2012. Diverse roles for semaphorin–plexin signaling in the immune system. *Trends Immunol.* 33:127–135. http://dx.doi.org/10.1016/j.it.2012.01.008

Tamagnone, L., S. Artigiani, H. Chen, Z. He, G.I. Ming, H. Song, A. Chedotal, M.L. Winberg, C.S. Goodman, M. Poo, et al. 1999. Plexins are a large family of receptors for transmembrane, secreted, and GPI-anchored semaphorins in vertebrates. *Cell.* 99:71–80. http://dx.doi.org/10.1016/S0092-8674(00)80063-X

Teijeira, A., E. Russo, and C. Halin. 2014. Taking the lymphatic route: dendritic cell migration to draining lymph nodes. *Semin. Immunopathol.* 36:261–274. http://dx.doi.org/10.1007/s00281-013-0410-8

Tolias, K.F., J.G. Duman, and K. Um. 2011. Control of synapse development and plasticity by Rho GTPase regulatory proteins. *Prog. Neurobiol.* 94:133–148. http://dx.doi.org/10.1016/j.pneurobio.2011.04.011

Wang, L.H., R.G. Kalb, and S.M. Strittmatter. 1999. A PDZ protein regulates the distribution of the transmembrane semaphorin, M-SemF. *J. Biol. Chem.* 274:14137–14146. http://dx.doi.org/10.1074/jbc.274.20.14137

Wang, X., A. Kumanogoh, C. Watanabe, W. Shi, K. Yoshida, and H. Kikutani. 2001. Functional soluble CD100/Sema4D released from activated lymphocytes: possible role in normal and pathologic immune responses. *Blood.* 97:3498–3504. http://dx.doi.org/10.1182/blood.V97.11.3498

Weber, M., and M. Sixt. 2013. Live cell imaging of chemotactic dendritic cell migration in explanted mouse ear preparations. *Methods Mol. Biol.* 1013:215–226. http://dx.doi.org/10.1007/978-1-62703-426-5_14

Winberg, M.L., J.N. Noordermeer, L. Tamagnone, P.M. Comoglio, M.K. Spriggs, M. Tessier-Lavigne, and C.S. Goodman. 1998. Plexin A is a neuronal semaphorin receptor that controls axon guidance. *Cell.* 95:903–916. http://dx.doi.org/10.1016/S0092-8674(00)81715-8

Witherden, D.A., M. Watanabe, O. Garijo, S.E. Rieder, G. Sarkisyan, S.J. Cronin, P. Verdino, I.A. Wilson, A. Kumanogoh, H. Kikutani, et al. 2012. The CD100 receptor interacts with its plexin B2 ligand to regulate epidermal γδ T cell function. *Immunity.* 37:314–325. http://dx.doi.org/10.1016/j.immuni.2012.05.026

Wolters, V., C. Krasel, J. Brockmann, and M. Bünemann. 2015. Influence of $G\alpha_q$ on the dynamics of M_3-acetylcholine receptor–G-protein–coupled receptor kinase 2 interaction. *Mol. Pharmacol.* 87:9–17. http://dx.doi.org/10.1124/mol.114.094722

Worzfeld, T., and S. Offermanns. 2014. Semaphorins and plexins as therapeutic targets. *Nat. Rev. Drug Discov.* 13:603–621. http://dx.doi.org/10.1038/nrd4337

Worzfeld, T., J.M. Swiercz, M. Looso, B.K. Straub, K.K. Sivaraj, and S. Offermanns. 2012. ErbB-2 signals through Plexin-B1 to promote breast cancer metastasis. *J. Clin. Invest.* 122:1296–1305. http://dx.doi.org/10.1172/JCI60568

Xia, J., J.M. Swiercz, I. Bañón-Rodríguez, I. Matković, G. Federico, T. Sun, T. Franz, C.H. Brakebusch, A. Kumanogoh, R.H. Friedel, et al. 2015. Semaphorin-plexin signaling controls mitotic spindle orientation during epithelial morphogenesis and repair. *Dev. Cell.* 33:299–313. http://dx.doi.org/10.1016/j.devcel.2015.02.001

Yazdani, U., and J.R. Terman. 2006. The semaphorins. *Genome Biol.* 7. http://dx.doi.org/10.1186/gb-2006-7-3-211

Yu, L., Y. Zhou, S. Cheng, and Y. Rao. 2010. Plexin A-semaphorin-1a reverse signaling regulates photoreceptor axon guidance in *Drosophila*. *J. Neurosci.* 30:12151–12156. http://dx.doi.org/10.1523/JNEUROSCI.1494-10.2010

Yukawa, K., T. Tanaka, K. Yoshida, N. Takeuchi, T. Ito, H. Takamatsu, H. Kikutani, and A. Kumanogoh. 2010. Sema4A induces cell morphological changes through B-type plexin-mediated signaling. *Int. J. Mol. Med.* 25:225–230.

Žárský, V., and M. Potocký. 2010. Recycling domains in plant cell morphogenesis: small GTPase effectors, plasma membrane signalling and the exocyst. *Biochem. Soc. Trans.* 38:723–728. http://dx.doi.org/10.1042/BST0380723

Zegers, M.M., and P. Friedl. 2014. Rho GTPases in collective cell migration. *Small GTPases.* 5. http://dx.doi.org/10.4161/sgtp.28997